VOT 71955

GRID MAT METHOD TO INCREASE THE BEARING CAPACITY OF SUBGRADE SOIL

(KAEDAH HAMPARAN GRID UNTUK MENAMBAHKAN KEUPAYAAN GALAS BAGI SUB-GRED TANAH)

AMINATON MARTO
FAUZIAH KASIM

RESEARCH VOTE NO:
71955

Jabatan Geoteknik dan Pengangkutan
Fakulti Kejuruteraan Awam
Universiti Teknologi Malaysia

2007

UNIVERSITI TEKNOLOGI MALAYSIA
Research Management Centre

PRELIMINARY IP SCREENING & TECHNOLOGY ASSESSMENT FORM

(To be completed by Project Leader submission of Final Report to RMC or whenever IP protection arrangement is required)

1. PROJECT TITLE IDENTIFICATION :

GRID MAT METHOD TO INCREASE THE BEARING CAPACITY OF SUBGRADE SOIL

Vote No: 71955

2. PROJECT LEADER :

Name :

MRS. FAUZIAH BTE KASIM

Address :

FACULTY OF CIVIL ENGINEERING, UNIVERSITI TEKNOLOGI MALAYSIA, 81310
UTM-SKUDAI JOHOR

Tel : 07-5531586 Fax : - e-mail : fauziah@fka.utm.my

3. DIRECT OUTPUT OF PROJECT *(Please tick where applicable)*

Scientific Research	Applied Research	Product/Process Development
☐ Algorithm	☑ Method/Technique	☑ Product / Component
☑ Structure	☐ Demonstration / Prototype	☐ Process
☐ Data		☐ Software
☐ Other, please specify	☐ Other, please specify	☐ Other, please specify
_____	_____	_____
_____	_____	_____
_____	_____	_____

4. INTELLECTUAL PROPERTY *(Please tick where applicable)*

☑	Not patentable	☐	Technology protected by patents
☐	Patent search required	☐	Patent pending
☐	Patent search completed and clean	☐	Monograph available
☐	Invention remains confidential	☐	Inventor technology champion
☐	No publications pending	☐	Inventor team player
☐	No prior claims to the technology	☑	Industrial partner identified

5. LIST OF EQUIPMENT BOUGHT USING THIS VOT

EQUIPMENT	SERIAL NUMBER
Plywood	**-**
Perspex	**-**
Silicon Sealant	**-**
Bolt and Nut	**-**

6. STATEMENT OF ACCOUNT

a) APPROVED FUNDING RM : 20,000.00

b) TOTAL SPENDING RM : 18,648.50

c) BALANCE RM : **1,351.50**

7. TECHNICAL DESCRIPTION AND PERSPECTIVE

Please tick an executive summary of the new technology product, process, etc., describing how it works. Include brief analysis that compares it with competitive technology and signals the one that it may replace. Identify potential technology user group and the strategic means for exploitation.

a) Technology Description

The finding presents additional information on soil reinforcement, especially for Malaysian soft soil. In addition techniques of laboratory scale test of grid model construction are presented for the development of the soil reinforcementtechnology in Malaysia.

b) Market Potential

Potential technology user groups include construction and consulting personnel or companies associated with soft soil technology in Malaysia and others related countries having problems in construction on soft soil. Techniques can be transferred commercially to other research organization.

c) Commercialisation Strategies

Technology

i) Presentation of finding in national and international conferences

ii) Technical talks to research personnel engineers (construction and consultants) and government authorities in construction and implementation

8. RESEARCH PERFORMANCE EVALUATION

a) FACULTY RESEARCH COORDINATOR

Research Status	( )	( )	( )	( )	( )	( )
Spending	( )	( )	( )	( )	( )	( )
Overall Status	( )	( )	( )	( )	( )	( )
	Excellent	Very Good	Good	Satisfactory	Fair	Weak

Comment/Recommendations :

_____

_____

_____

_____

_____

…… Name : ……..

Signature and stamp of Date : ……

JKPP Chairman

b) RMC EVALUATION

Research Status	( )	( )	( )	( )	( )	( )
Spending	( )	( )	( )	( )	( )	( )
Overall Status	( )	( )	( )	( )	( )	( )
	Excellent	Very Good	Good	Satisfactory	Fair	Weak

Comments :-

_____

_____

_____

_____

_____

_____

Recommendations :

☐ Needs further research

☐ Patent application recommended

☐ Market without patent

☐ No tangible product. Report to be filed as reference

…….. Name : …….

Signature and Stamp of Dean / Deputy Dean Research Management Centre

Date :…….

UNIVERSITI TEKNOLOGI MALAYSIA

BORANG PENGESAHAN
LAPORAN AKHIR PENYELIDIKAN

TAJUK PROJEK : **GRID MAT METHOD TO INCREASE THE BEARING CAPACITY OF SUBGRADE SOIL**

Saya **PN. FAUZIAH BTE KASIM**
(HURUF BESAR)

Mengaku membenarkan **Laporan Akhir Penyelidikan** ini disimpan di Perpustakaan Universiti Teknologi Malaysia dengan syarat-syarat kegunaan seperti berikut :

1. Laporan Akhir Penyelidikan ini adalah hakmilik Universiti Teknologi Malaysia.
2. Perpustakaan Universiti Teknologi Malaysia dibenarkan membuat salinan untuk tujuan rujukan sahaja.
3. Perpustakaan dibenarkan membuat penjualan salinan Laporan Akhir Penyelidikan ini bagi kategori TIDAK TERHAD.
4. * Sila tandakan (/)

☐	SULIT	(Mengandungi maklumat yang berdarjah keselamatan atau Kepentingan Malaysia seperti yang termaktub di dalam AKTA RAHSIA RASMI 1972).
☐	TERHAD	(Mengandungi maklumat TERHAD yang telah ditentukan oleh Organisasi/badan di mana penyelidikan dijalankan).
☑	TIDAK TERHAD	

TANDATANGAN KETUA PENYELIDIK

PN. FAUZIAH BTE KASIM
Nama & Cop Ketua Penyelidik

Tarikh : **23 November 2007**

CATATAN : ***** *Jika Laporan Akhir Penyelidikan ini SULIT atau TERHAD, sila lampirkan surat daripada pihak berkuasa/organisasi berkenaan dengan menyatakan sekali sebab dan tempoh laporan ini perlu dikelaskan sebagai SULIT dan TERHAD.*

ACKNOWLEDGEMENTS

The author is grateful to Research Management Center (RMC), UTM for giving the grant of this research and also to Universiti Teknologi Malaysia (UTM) for helping us in management part of this research.

The author wishes to thank all technicians of Geotechnic Lab, Fakulti Kejuruteraan Awam, UTM especially to En. Abdul Samad Salleh, En. Zulkifly Wahid, En. Kamarulzaman Ismail and En. Sahak Tokol for helping the researhers during the experimental work.

The author would like to express her thanks to all researcher for their continous support throughout the work especially to Assoc. Prof. Dr. Aminaton Marto, En. Anwar Khatib, En. Badrul Hisham Hasbi and Pn. Rozaini Md. Ribi for their inspiration, encouragement and continued guidance throughout the various stages of this research.

GRID MAT METHODS TO INCREASE THE BEARING CAPACITY OF SUBGRED SOIL

(Keywords: Bearing Capacity, Soft Soil, Grid Models, Settlement)

The investigation will be conducted on cohesive soil produced from kaolin powder. The grid mat will made by different shapes, i.e., triangular and square, and made of materials such as steel. Each model testing will consist of two stages; consolidation stage and loading stage. In the consolidation stage, the soil will be double drained whereby the loading plate will be drilled to from holes of about 5mm diameter so that drainage can occur through the loading plate as well. During loading stage, the soil deformation is to be monitored using at least two LVDT while the loading is measured using the load cell attached at the top loading platen. The LVDT and the load cell will be attached to a readout unit which will either be a data logger or an ADU connected to a computer. Different shapes of grid mat will be loaded till failure and the one that can give the highest value will be the best solution to be used to improve subgrade of highway. Besides giving high bearing capacity, grid mat can also occasionally reduce differential settlements, which are normally present in soft soils. Through attaching grid at the base of the foundation, the performance characteristics of the grid mat could be modified. This modification produces a new type of foundation known as “grid mat foundation” that could withstand higher load than the others foundation. The results showed that the diamond pattern grid mat models gave higher ultimate bearing capacity with less settlement as compared to the others grid mat models, with maximum axial force value 188 N for diamond pattern, 180 N for square pattern and 182 N for chevron pattern. The maximum axial force value is the higher the ultimate bearing capacity and the lower the settlement will be.

Key Researcher:

Assoc. Prof. Dr. Aminaton Marto
Ms Fauziah Kasim
Mr. Anwar Khatib

Email: aminaton@utm.my, fauziah@fka.utm.my
Tel. No.: 07-5537781 / 31586
Vot No.: 71955

KAEDAH HAMPARAN GRID UNTUK MENAMBAHKAN KEUPAYAAN GALAS BAGI SUB-GRED TANAH

(Kata Kunci:Keupayaan Galas, Tanah Lembut, Model Grid,Enapan)

Penyiasatan akan dilakukan ke atas tanah jelekitan yang dihasilkan daripada serbuk kaolin. Hamparan grid diperbuat dalam bentuk segitiga dan segiempat, serta diperbuat daripada bahan seperti keluli. Setiap model ujian mengandungi dua peringkat iaitu peringkat pengukuhan dan peringkat pembebanan. Dalam peringkat pengukuhan tanah akan menjadi dua aliran dimana plat pembebanan akan ditebuk untuk membentuk lubang 5mm diameter, kemudian pengaliran akan terjadi melalui plat pembebanan. Semasa peringkat pembebanan perubahan tanah hendaklah diawasi menggunakan sekurang-kurangnya 2 LVDT sementara beban pula ditentukan menggunakan sel beban yang dilampirkan pada atas plat pembebanan. LVDT dan sel beban akan dilampirkan untuk mengeluarkan bacaan unit yang akan menjadi samada *Data Longger* atau ADU yang disambung ke komputer. Bentuk hamparan grid yang berbeza akan dibebankan sehingga gagal dan nilai yang tertinggi akan digunakan sebagai penyelesaian terbaik untuk memperbaiki sub-gred bagi lebuhraya. Selain memberikan keupayaan galas yang tinggi, ia juga boleh mengurangkan enapan yang berlainan, yang mana biasanya terjadi pada tanah lembut. Melalui sentuhan grid pada dasar asas, ciri-ciri kelakuan bagi hamparan grid boleh diubahsuai. Pengubah suaian ini menghasilkan sejenis asas baru yang dikenali sebagai ”asas hamparan grid” yang boleh menahan beban lebih daripada asas lain. Keputusan menunjukkan bahawa model hamparan grid memberikan keupayaan galas muktamad yang tinggi dengan enapan yang kurang berbanding dengan model hamparan grid yang lain, dengan nilai daya maksimum 188 N bagi brntuk ”diamond”, 182 N bagi bentuk ”chevron” dan 180 N bagi bentuk Segiempat. Nilai daya maksimum menunjukkan keupayaan galas muktamad yang tinggi dan kurangnya enapan yang terjadi.

Key Researcher:

Assoc. Prof. Dr. Aminaton Marto
Ms Fauziah Kasim
Mr. Anwar Khatib

Email: aminaton@utm.my, fauziah@fka.utm.my
Tel. No.: 07-5537781 / 31586
Vot No.: 71955

TABLE OF CONTENTS

LIST OF TABLE

LIST OF FIGURE

LIST OF SYMBOL

c	-	Cohesion value of soil
ϕ	-	Angle of internal friction of soil
σ_n	-	Normal stress due to applied vertical load
τ_f	-	Shear stress at failure of soil
τ	-	Shear stress of soil
S_u	-	Undrained shear strength
σ'_{vc}	-	Vertical consolidation stress
σ_1	-	Major principal stress
σ_2	-	Intermediate principal stresses
σ_3	-	Minor principal stresses
Gs	-	Specific gravity of soil
e_o	-	Initial void ratio of soil

LIST OF APPENDIXS

CHAPTER 1

INTRODUCTION

1.1 Introduction

Construction of a structure on soft soils will always be a problem to civil engineers. Besides having low bearing capacity, soft soils are also high in compressibility that may result in large settlement, both total and differential settlement. However, experience with this kind of structures in Indonesia shows that large differential settlement still occur causing cracks to the building and even failure to the structure, Marto et al. (1999). By attaching grids of certain length to the base of the raft foundation, higher bearing capacity and smaller settlement may be achieved, compared to the conventional raft foundation.

According to Broms and Massarch (1997), failure of the grid mat units in clay can be caused by two different mechanisms. Firstly, the penetration failure, governs when the height of the cells is relatively small in comparison with the circumference of the individual cells. Secondly, the bearing capacity failure, governs when the height of the cell is relatively large. In the latter case, the friction or the adhesion of the soil along the vertical plates is sufficient to prevent the extrusion of the soil through the cells

The grid mat methods are usually well suited for various offshore structures (e.g. drilling platforms, lighthouse) and highway. The foundation elements which are used in this method are commons proposed of open triangular, square or circle cells which are joined together to form a grid. The grid mat can be adjusted to fit different bottom conditions. When the soil consists of dense sand or stiff to hard clay and it is possible to push the grid into the soil, they can be placed directly on the bottom and the open cells are then filled with sand, gravel or rockfill. In soft clay or in loose sand the grids are pushed into the soil. If the bearing capacity of the soil is very low, the grids are combined with piles.

1.2 Background of study

Soft cohesive clays are normally associated with large settlement and low shear strength. Various techniques are available to reduce the settlements. It is not economically feasible to excavate a thick stratum of very soft clay some tens of meters deep and replace it with suitable fill for highway construction. A more cost effective but still an expensive treatment will be the construction of the pavement on reinforced concrete slabs supported on pile driven to set into a stiff underlying stratum. A much cheaper but probably unsatisfactory solution will be the used of grid mat as separator and reinforcement to increase the bearing capacity of the soil. With very weak soil and the limited bearing capacity commensurate with the maintenance of structural integrity of the asphaltic surfacing of the overlaid pavement may prove to be low to confer any advantage to the use of grid mat.

Several investigation have reported the beneficial use geocells. Rea and Mitchel (1978), and Mitchel et. al. (1979) conducted series of model plate load tests on circular footings supported over sand-filled square shape paper grid cells to identify different modes of failure and arrive at optimum dimensions of the cell. Schimizu and Innui (1990), carried out load test on single six-side cell of geotextile wall buried in the subsurface of the soft ground. Krishnaswamy te. el, (2000) have

conducted lad tests on geocell supported model embankments over soft clay foundation. Cowland and Wong (1993), reported case studies on geocell mattress supported road embankment. Bush et. al. (1990) have proposed a methodology to calculate the increase in bearing capacity of the soft soil due to the presence of geocell mattress on the top of it. Dash, Krishnaswamy, and Rajagopal, (2001), explain that the better improvement in the performance of footing can be obtained by filling the geocell with denser soils because of dilation induced load transfer from soil to goecell. The optimum aspect ratio of geocell pockets for supporting was found to be around 1.67.

The design approach consists of selecting an economical embankment slope and the reinforcement which will make the embankment safe in the four modes of failure, (Shenbaga R.Kaniraj, 1988). According to Broms and Massarch (1977), the failure of a grid mat in clay can be caused by two different mechanism. The first failure mode, namely penetration mode occurs when the height of the cell is relatively small in comparison with the circumference of the individual cells. The second failure mode, namely bearing capacity failure, occurs when the height of the cells is relatively large. Then the friction or the adhesion of the soil along the vertical plates is sufficient to prevent the extrusion of the soil through the cells.

1.3 Statement of Problem

The advancement of works in bearing capacity studies have lead to further works on the used of reinforcement in soft soils or clays. Soft clays have been known to cover vast coastal areas of Malaysia. As development progress, more constructions areas have occupied these compounds. The problem with soft clay, as reported earlier, has been large settlement and low bearing capacity. With more research being conducted, various techniques are available to reduce the settlement and increase the bearing capacity of soft soil. It is hope that this research will give a new alternative for a cost effective solution for bearing capacity problem of soft clay.

1.4 Objective and Scope of Study

The main objective of this study are:

1. To determine the shape of the grid mat that will give the highest bearing capacity
2. To determine the effect of the grid mat on settlement and bearing capacity of subgrade soil on different shape.

This study presented effect of the use of grid mat for increasing bearing capacity and decreasing settlement. However, the study only consider the placement of the grid mat on soil surface.

1.5 Significance of Study

The significance of this study are:

1. The study can be approach to increase the bearing capacity and reduce settlement on the sub grade soil.
2. This study will be probably give another alternative for new type of soil stabilisation method especially in the construction of highway or runway.
3. This study is important for the geotechnical engineers and soil development agencies to plan any construction involving soil reinforcement.

CHAPTER 2

LITERATURE REVIEW

2.1 Introduction

A review of previous research work in reinforcement on soft soil is presented in this chapter. The review is restricted primarily to problem under dynamic load. First, constitutive laws of soil will be presented, followed by a review of available reinforcement models. Reinforcement design is based on providing of transmitting the loads from a structure to the underlying soil without a soil shear failure (a plastic flow and or a lateral expulsion of soil from beneath the foundation) or causing excessive settlement of the soil under imposed loads. If both these requirements for a structure are not satisfied, the structure will, in general, perform unsatisfactorily. That is, it will settle excessively, tilt, end form unsightly cracks, and may even collapse if the differential settlements induce sufficient overstress in critical members. Finally previous experimental work on this field is reviewed in this chapter.

2.2 Review on Soil Reinforcement

Arenicz, (1992) the use of ribbed rather than smooth strips as soil reinforcement was found to be superior in enhancing soil shear strength. However that the comparable effectiveness of strip ribs in generating extra strength of soil seem to decline with the use of wider strips. The results indicate the importance of reinforcement layout in soil shear strength enhancement. Kaniraj, (1988), in the design of such reinforced embankments, four potential modes of failure should be investigated. These are, bearing capacity failure, sliding failure, foundation soil squeezing failure and rotational failure. The design consists of selecting an economical embankment slope and the reinforcement which will make the embankment safe in the four modes failure. Haliburton et al. (1978) assumed that the construction cost for the fabric-reinforcement was approximately 60% of the estimated cost of construction with the end dumping displacement method of dike construction, then Marto et al. (1999) have assumed that the higher rib ratio will be increase the bearing capacity and the lower be settlement.

Shin, et. al (1993) on the laboratory test were conducted to determine the critical non dimensional values for the depth and width of the geogrid reinforcement layer and also the location of the first layer of geogrid with respect to the bottom of the foundation to obtain the maximum possible bearing capacity ratio. Geosynthetics are increasingly being used as reinforcement in permanent earth structures constructed in conjunction with transportation facilities (Tatsouka and Leshchinsky 1993), including retaining wall, steep slopes and bridge abutments. In many cases, the inclusion of geosynthetics in soils allows construction of structures at significantly reduced cost as compared to unreinforced soil structures. Then Min, et. al. (1995) assumed that the ultimate pullout load and interaction coefficient, Ci, obtained from repeated loading tests were about 20% less than the values obtained from sustained loading tests. This suggests that a Ci smaller than that obtained in static (conventional) tests should be used in structures subjected to dynamic load.

The classical bearing capacity theory for flat foundations was extended for triangular shell strip footings, and design chart for the modified bearing capacity coefficients are presented for the triangular case. Although there have been rapid advances in efficiency, reliability and economy in the fields of construction technology and assembly of precast concrete units, (Hanna et.al. 1990).

Shell foundations are capable of supporting higher vertical load, produce lesser settlement, and are economical in terms of material. However, through experimental data, the actual distribution of the contact pressure on the soil is found to be function of the cell-soil interaction, and is far from being uniform (Kurian, 1981).

A reinforced earth slab consists of a bed of granular soil strengthened by horizontal layers of flat metal strips or ties with relatively high tensile strength and developing good frictional bond with the soil. Many other studies have described this type of soil-reinforcing, principally in connection with retaining; (Richardson et, al, (1975). Then Jean Binquet, et. al (1976a) and Binquet, et. al (1976b) assumed that the basic to the method is assumed ability to calculate the load-settlement and ultimate bearing capacity of a strip footing of the same size on unreinforced soil. Therefore, the reliability of the load-settlement or ultimate bearing capacity design for the reinforced soil can be no more accurate than the reliability of settlement and bearing capacity predictions for regular footings. Verma, and Char, (1986) in the bearing capacity on model footings on sand subgrades reinforced with galvanized rods placed vertically in the subgrade have shown beneficial effects of reinforcement.

According Fatani, et. al (1991)., the reinforcement elements consisted of flexible, semi rigid, and rigid metallic fibers. The orientations of the fibers to the shear plane were varied and had a marked effect on the shear resistance. Increases in peak and residual strengths of 100 and 300%, respectively were observed over unreinforced sand. Specimens reinforced with randomly oriented flexible fibers also exhibited a similar improvement of strength parameters. Akinmusuru, et, al (1981) in

the results obtained have the shown that the bearing capacity of a footing depends on the horizontal spacings between strips, vertical spacing between layers, depth below the footing of the first layer, and number of layer of reinforcement, the bearing capacity values can be improved by a factor of up to three time that of the unreinforced soil. However, practical considerations could limit suitable arrangements to bearing capacity improvement factor of about two.

The undrained behaviour of embankments constructed on soft cohesive deposits is examined for the case where the embankment is reinforced using steel strips. A finite-element analysis that consider plastic failure of the fill and the foundation, pullout of steel strips, and potential yield of the reinforcement is used to demonstrate how steel reinforcement can improve embankment stability. The effect of strip spacing on the mode of failure and embankment stability is examined for a range of soil strength profiles that involve an increase in undrained shear strength with depth, (Rowe, and Mylleville Brian, 1993).

Laboratory model test result for the ultimate bearing capacity of strip and square foundations supported by sand reinforced with geogrid layers have been presented. Based on the model test results, the critical depth of reinforcement and the dimensions of the geogrid layers for mobilizing the maximum bearing-capacity ratio have been determined and compared, (Omar, Das, and Yen, 1993)

Maher, and Ho, (1993), assumed that the test results indicated that the fiber reinforcement significantly increases the compressive and splitting tensile strength of the cemented sand. An increase in the compressive and tensile strength was found to be more pronounced at higher fiber contents and longer fiber length. Peak strength envelopes in compression indicated that both the friction angle and cohesion intercept of cemented sand were increased as a result of fiber inclusion. Fiber reinforcement als affected the response of cemented sand to cyclic load by significantly increasing the number cycles, and the magnitude of cyclic strain needed to reach failure.

Chalaturnyk, et, al (1990) through increased confining stresses on the soil within the reinforced slope, the soil strength required to maintain equilibrium was reduced. The horizontal stiffness provided by the reinforcement led to significant reduction in horizontal strains and deformations and moderate reductions in vertical strains and deformations.

The principal tensile strains within the reinforced slope were reduced substantially but no reorientation of the principal tensile strains axes resulted due to the presence of the reinforcement. The finite element analysis of the reinforced embankment construction gives the magnitude and distribution of load within the reinforcement. For all embankment heights, the maximum reinforcement load did not occur in the lowest reinforcing layer but in the reinforcing layer placed 0.4H above the foundation, where H is the height of the slope.

Milovic, (1977) assumed that the load tests have been carried out without reinforcement and with two and three layers of reinforcing, where the polypropilen codrds of 15 mm in diameters were used. The obtained model and field load test results indicate the advantages and possibilities for improvements in the load settlement and ultimate bearing capacity of footing on granular soils. Considerable decreasing of settlements in the reinforced soil in comparison with the unreinforced soil represents an important advantage for the practice.

Marto, et al,(2000) the efficiency towards loading and towards settlement for ribbed raft foundation models are found to be of second degree polynomial equation. The efficiencies increase with the rib ratio (H/B) for all LB ratio, both for models tested an sandy clay than on marine clay. However the efficiencies are better for model tested on sandy clay than marine clay.

2.2.1 Geogrids

The relatively recent discovery of methods of preparing high modulus polymer materials by tensile drawing (Capaccio, et. al, 1974), in sense "cold working", has raised the possibility that such materials could be used in the reinforcement of a number of construction materials, including soil. Today, the major function of such geogrids is in the area of reinforcement. This area, as in many others, is very active, with a number of different style, materials, connection, etc., making up today's geogrid market. The key feature of geogrids is that the openings between the longitudinal and transverse ribs, called the "apertures" are large enough to allow soil strike-through from one side of the geogrid to the other. The ribs of geogrids are often quite stiff compared to the fibers of geotextiles. Geotextiles are being increasingly used in road construction, tank foundation and several other reinforcement (tensile or tensioned members) applications. Numerous pavement design methods have been suggested (Giroud, and Noilray, 1981., Sellmeijer et. al, 1982, and Milligan et. al, 1989), for unpaved roads which are characterized by high allowable rut depths, low volume of traffic and no vehicle wander.

Nagaraju and Mhaiskar (1983), have suggested the use of soil filled tubes for paved roads, while Kazerani and Jamnejad, (1987) have segested the use of geocell for paved road. De Garided et. al, (1986),have used geocells of width (a) and height (b) ratio (ie. alb) of 0.5 and reported that the bearing capacity can be improved up to three times. Several other investigators have reported the use of geocells or different a!b ratio with varying degrees of benefit. Bush et. al. (1990), have reported the use of geogrid geocell embankment on soft soil.

2.2.2 Geocell Mattress

Geocell mattress is a 1m deep open cellular structure constructed from a biaxial grid base layer with uniaxial grids forming vertical cells, which are then filled with graded granular fill. The geocell foundation mattress consists of a series of interlocking cells, constructed from polymer geogrids, which contains and confines the soil within its pockets. It intercepts the potential failure planes because of its rigidity and forces them deeper into the foundation soil, thereby increasing the bearing capacity of the soil.

The filled Geocell greates a rigid, high strength foundation for the embankment, a construction platform for earthworks plat, and drainage layer the base of the embankment, (Carter and Dixon, 1995). The Geocell provides a cost-effective alternative to removal and replacement of soft foundation soils which are underlain by firmer material. Potential failure planes are intersected and the rigidity of Geocell forces them deeper into firm strata. The critical failure mechanism becomes that of plastic failure of the soft layer. The rough interface at he base of the Geocell ensures mobilization of the maximum shear capacity of the foundation soil and significantly increases stability. Differential settlement and lateral spread are also minimized. Robertson and Gilchrist (1987), describe the design and construction of a Geocell to support a highway embankment over very soft ground on the A807 road at Auchenhowie near Glasgow. Here a 4.5 m high embankment was constructed on a 4.0 m thick layer of soft silty clay with an average undrained cohesion of 15 kN/mZ underlain by stiffer material. The use of a Geoceoll represented a saving of 31 % over the excavation and replacement option. Construction of the Geocell was carried out in very poor conditions during the winter of 1985/86. The Geocell enabled the overlying embankment to be constructed rapidly. Performance since construction has been good.

2.3 Previous Study on Reinforced Soil Composites

By suitably mixing soil and polymer element(s), a reinforced soil composite results. The interesting system are described:

2.3.1 Discontinuous Fiber and Meshes

Fiber reinforcement has long been use to enhance the brittle nature of cementatious materials, so it should come as no surprise that similar attempts should be made with polymer fiber in soil. Most-work has been done with cohesionless sand and gravels, but cohesive silt and clays might benefit as well. Based on laboratory tests, Gown, et al. (1985), have found that mesh element in 1.18% weight proportion resulted in an apparent cohesion of 7.3 lb/in2 (SOkPa) for granular soil. What is optimal behavior for different soils, different fiber or meshes, different sizes and percentages of fibers or meshes.

2.3.2 Continuous Fibers

Laflaive, (1982), has pioneered the application of mixing continuous polyester threads with granular soil to steepen and/or stabilized embankments and slopes. The technique, called Texol, uses a specially designed machine capable of dispensing 23 yd 3/hr. (30m3/hr) of soil mixed with the fibers coming from 40 bobbins, resulting in a weight percent of 0.1 to 0.2%. The finished fiber-reinforced soil has fascinating properties. The system has been used in France where higway slopes of 69 deg, have been constructed and have remained stable. Large field trials with enormous surcharges have failed to destroy the thread-reinforced soil mass. What failures that have resulted are mass failures behind the reinforced zone. Laboratory studies on

continuous fiber reinforced granular soil have resulted in apparent cohesion values in excess of 15 Win 2or 100 kPa, (Laflaive, 1986). Use of the technique in the widening of highways or railroads that are in cut areas is quite attractive.

2.3.3 Three Dimensional Cells

Rather than rely on friction, arching, and entanglements of fiber or mesh for improved soil performance, geosynthetics can be formed to physically contain soil. Such containment, or confinement, is known to vastly improve granular soil shear strength, as any triaxial shear test will substantiate. Furthermore, the increased shear strength due to confinement will provide excellent bearing capacity.

The U. S. Army Corps of Engineers (1981), in Vickburg, Mississippi , has experimented with a number of confining systems, beginning with short pieces of sand-filled plastic pipes standing on end, to cubic confinement cells made from slotted aluminum sheets, to prefabricated polymeric systems called sand grids or geo cells. Currently these system s are made from high-density polyethylene (HDPE) strips 8 in. (200mm) wide and approximately 50 mils (1.2 mm) thick. They are ultrasonically welded along their 8 in.(200 mm) width at approximately 13 in (33 cm) intervals and are shipped to the job site in a collapsed configuration..

In term of design, cuch system are quite complex to asses. If one adapts the conventional plastic limit equilibrium mechanism as use in statically loaded shallow foundation bearing capacity, its failure mode is interrupted by the vertically deployed strips. For such a failure to occur, the sand in a particular cell must overcome the side fiiction, punch out of it, thereby loading the sand beneath the level of the mattress. This in turn, fails bearing capacity, but now with the positive effects of a surcharge loading and higher density conditions. The relevant equations are as followed by an example:

Without mattress:

$$P = cN_c\xi_c + qN_q\xi_q + 0.5\gamma BN_\gamma\xi_\gamma \quad (2.4)$$

With mattress:

$$P = 2\tau + cN_c\xi_c + qN_q\xi_q + 0.5\gamma BN_\gamma\xi_\gamma \quad (2.5)$$

Where:

p : the maximum bearing capacity load (= tire inflation pressure of vehicles driving on system if this the application)

c : the cohesion (equal to zero when considering granular soil such as sand)

q : The surcharge load (=ygD,)

y_q : the unit weight of soil within geocell

D_q : the depth of geocell

B : the width of applied pressure system

y : the unit weight of soil in failure zone

N_c, N_q, N_γ : the bearing capacity factors, which are functions of ~ (where ~ = the angle of shearing resistance (frictionangle) of soil; see any geotechnical engineering text, e.g., Koerner (1984).

ξ_c, ξ_q, ξ_γ : the shape factor used to account for differences in the plane strain assumption of the original theory

τ : the shear strength between geocell wall and soil contained within $\tau = \sigma_h \tan \delta$ (for granular soil)

σ_h : the average horizontal force within the geocell ($\approx pK_a$)

p : applied vertical pressure

K_a : The coefficient of active earth pressure = tan 2(45 - ~/2), for Rankine theory

δ : the angle of shearing resistance between soil and cell wall material (≈18 deg. Between sand and HDPE, ≈35 deg. Between sand and nonwoven geotextile).

2.3.4 Three Dimensional Mattresses

A deeper, more rigid mattress can be developed by a three dimensional geosynthetic structure consisting, for example, of gravel-filled geogrid cells. These cells are typically 3 ft. (1 m) deep and can be either square or triangular in plan view. They are joined together by an interlocking knuckle joint with a steel or PVC rod threaded through the intersection forming the coupling. This is called a "bodkin" joint. Both Tensar and Tenax can be joined in this manner. Other geogrids can be joined by hog ring or other suitable fasteners, (Koerner, 1990).

Edgar (1984) reports on a three dimensional geogrid mattress that somewhat parallels the goecells, the soil-filled geogrid mattress was constructed over soft fine-grained soils. On top of it was successfully placed a 50-ft. high embankment. It was felt that the reinforced slip plane was forced to pass vertically through the mattress and therefore deeper into the stiffer layers of the underlying subsoils. This improved the stability to the point where the mode of failure was probably changed from a circular arc to a less critical plastic failure of the soft clay.

2.4 Application of Geogrid Reinforcement

Since the primary function of geogrids is invariably reinforcement, this section will proceed from one application area to another. The order will parallel that of the section on geotextile reinforcement, with the addition of areas unique to geogrid.

2.4.1 Unpaved Roads

The use of geogrids to reinforce soft and/or compressible foundation soils for unpaved aggregate roads is a major application area. Many successes havce been reported, together with several attempts at a design method. By far the most advanced analytical method, and the one that will be used here. (Giroud, Ah-Line , and Bonaparte, 1984). The method follows along lines similar to those described in the geotextile section on unpaved roads. The nonreinforced situation is first handled, and then new concepts are developed for the reinforced case. Here the mechanisms of reinforcement are increased soil strength, load spreading, and membrane support via controlled rutting. The difference in required thickness of stone base is thereby obtained and then compared to the cost of the geogrid. If the latter is less expensive (as it usually is for soil sub-grade CBR value less than 3). For the geogrid reinforce case, new concepts are developed that include the three above-mentioned beneficial mechanism attributed to inclusion of the geogrid, (Koerner, 1990). Their effect are as follow:

a An increase in soil subgrade strength from the nonreinforced case to the reinforced case as indicated in the following equations:

$$P_e = \pi C_{un} + \gamma h_o \qquad (2.1)$$

$$P_{lim} = (\pi + 1)\, c_{un} + \gamma h \qquad (2.2)$$

where:

P_e : the bearing capacity pressure based on the elastic limit (nonreinforced case)

P_{lim} : the bearing capacity pressure based on the plastic limit (reinforced case)

γ : the unit weight of aggregate

h_o : the aggregate thickness without reinforcement

h : the aggregate thickness with reinforcement

b : An improved load distribution to the soil subgrade due to load spreading, which is quantified on the basis of pyramidal geometric shape.

c : A tensioned membrane effect, which is a function of the tensile modulus and elongation of the geogrid and the deformed surface of the subgrade soil, i.e., the rut depth.

2.4.2 Embankment and Slopes

The use of geogrids to reinforce sloping embankments directly parallels the techniques and designs that were developed using geotextiles. The use of limit equilibrium via a circular arc failure plane, thereby intercepting the various layers of reinforcement. This allowed for the formation of a factor of safety expression as follows:

$$Fs = \frac{M_R + \Sigma^{m}_{i=1} T_i Y_i}{M_D} \qquad (2.3)$$

where

M_R : the moments resisting failure (due to soil stregth)

M_D : the moments driving (causing) failure e.g., gravitational, seepage, seismic, dead, and live loads)

T_i : the allowable reinforcement strength

Y_i : the appropriate moment arm(s)

M : the number of separate reinforcement layers

2.5 Effect of Grid Mat on Bearing Capacity and Pull-Out Strength

2.5.1 Axial Load Tests

The Bearing capacity of four models with triangular or square cells and of triangular and rectangular mono cells were investigated as well as the bearing capacity of plates of the same shape and size as the models. The tests were carried out in both loose and dense sand. The height of the sand fill within and around the models was changed as well as the penetration depth of the models. The deformation rate was kept constant during each test (about 2cm/min). In some of the tests the sand in the cells was compacted. The shape of the load-displacement relationships when the grids were placed directly on the surface is illustrated in Figure 2.5. It can be seen that the relative density of the soil below the grid has large effect on the load-deformation relation-ship. The resistance increased expotentially with increasing penetration depth.

The soil penetration at first into the cells. The friction resistance along the cell walls increased gradully until the surface area of the cells in contact with the soil was large enough to resist the relative movement of the soil. The grid behave then as a solid plate and the grid with the enclosed soil moved down as a unit.

The Penetration Depth required to reach the ultimate bearing capacity of the soil was approximately twice the cell width when the cells were square and approximately the cells width when the cells were triangular.

Typical load-displacement relationships when the cells were filled with sand or when the grid was pushed in to the underlying soil are shown in Figure 2.6. The grid and the soil within the cells moved down together as a unit. The axial displacement required to reach the ultimate bearing capacity of the soil was small

compared to the case when the grid was placed directly on the surface. The penetration resistance increased rapidly with increasing dispplacement.

It can be seen from Figure 2.6 that the relative density of the soil had a large effect on the load-displacement relationship. The ultimate bearing capacity increased rapidly as the density of the soil increased.

The penetration is affected considerably by the value of the coefficient of lateral earth pressure, K. This coefficient varied between 0.75 and 0.85 for the grid with rectangular cells when the soil in the cell was dense. The corresponding variation for the grids with triangular cells was between 0.55 and 0.65 when the soil was loose, and 0.65 and 0.75, when the soil was dense. The value of K was thus less for the triangular cells than for the rectangular cells.

Test result indicate furthermore that cyclic loading has a large influence on the settlements, while the ultimate bearing capacity bearing capacity is hardly affected. The settlement increased with increasing load level. The increase was two to four times after 1000 load cycles when the maximum level of the cyclic loading increased from 50% to 90% of the static failure load.

2.5.2 Pull-Out Tests

The pull-out resistance was also investigated. The height of the sand fill within and around the models was varied as well as the relative density of the sand. Typical load displacement relationships from the pull-out tests are shown in Figure 2.7. The height of fill in the cells was 10 cm. It can be seen that a very small displacement less than 1 mm was required to mobilize the maximum resistance. The resistance decreased approximately linearly with increasing displacement as the

contact area of the cell walls with the soil decreased. The pull-out resistance was in most cases approximately equal to the weight of the soil enclosed in the grid.

The pull-out resistance increased in general with increasing total mantel area (A_m) in contact with the soil and the total bottom area (A_b). The pull-out resistance was approximately equal to the weight of the soil enclosed by the grid.

The tension tests indicate that the behaviour of the grids with triangular cells is superior to the grids with rectangular cells.the behaviour of the rectangular cells can be improved by attaching ribs to the lower edge of the grid. The tension tests show furthermore that the pull-out resistance of a grid with triangular cells is equal to the weight of the soil enclosed within the cells when the height (H) of the soil within the cells is at least equal to the width (L) of the cells.

The pull-out resistance was approximately equal to the weight of the soil enclosed within the grid except for the grids with square cells and when the height of the fill was small. The model tests also indicate that the behaviour of the grids with triangular cells was superior to the grids with rectangular or square cells both with respect to the load carrying capacity and the rigidity of the grid.

2.6 Bearing Capacity

In geotechnical engineering, bearing capacity is the capacity of soil to support the loads applied to the ground. Figure 2.8 shows the bearing capacity of soft soil. The bearing capacity of soil is the maximum average contact pressure between the foundation and the soil which will not produce shear failure in the soil. Ultimate bearing capacity is the theoretical maximum pressure which can be supported without failure; while allowable bearing capacity is the ultimate bearing capacity divided by a

factor of safety. Sometimes, on soft soil sites, large settlements may occur under loaded foundations without actual shear failure occurring; in such cases, the allowable bearing capacity is based on the maximum allowable settlement. There are three modes of failure that limit bearing capacity: general shear failure, local shear failure, and punching shear failure.

When the load is applied on a limited portion of the surface a soil, the surface settles. The relation between the settlement and the average load per unit of area may be represented by a settlement curve. The load per unit area of the foundation at which the shear failure in soil occurs is called the ultimate bearing capacity (Das, 1999).

According Koerner, (1984), the geogrid have been used to increase bearing capacity of poor soil in two ways:

a. as continuous sheet placed under stone base layers
b. as mattresses consisting of three-dimensional interconnected cell beneat5h embankments

The technical database for single-layer continuous sheets is being developed by Jarret, (1984) and by Milligan, and Love (1984), in both cases large-scale Laboratory tests are being used. Milligan, and Love (1984) work plotted in the conventional q/c_u versus ρ/β and also as $2/\sqrt{c_u}$ versus ρ/β. The latter graph is not conventional but does sort out the data nicely. Clearly shown in both instances is the marked improvement in load-carrying capacity with the geogrid at high deformation an the only nominal beneficial effect at low deformation.

Edgar, (1984) report on a three dimensional geogrid mattress tha somewhat parallels the geocell . The soil-filled geogrid mattress was constructed over soft fine-grained soils. A 50-ft.high embankment was successfully placed above the mattress.

It was felt that the reinforced slip plane was forced to pass vertically through the mattress and therefore deeper into stiffer layers of the under laying sub-soils. This improved the stability to the point where the mode of failure was probably changed from a circular arc to a less critical plastic failure of the soft clay.

2.6.1 Cohesionless Soil

According Brooms and Massarch, (1977), the ultimate bearing capacity is either governed by the penetration resistance of the grid or by the bearing capacity of the soil. The bearing capacity at penetration failure can be analyzed by considering the forces acting on a slice with the thickness d,, located at at a distance h below the surface of the soil as indicated in Figure 2.1 and Figure 2.2.

It has been assumed that the earth pressure distribution within the cells can be calculated by the same method as that used for soils. The pressure distribution and the penetration resistance are thus affected by the friction along the walls of the cells which increases with the overburden pressure and with increasing wall friction. The friction f along the perimeter of the slice can be calculated in terms of effective stress from :

$$f = K\sigma_v tg\Phi_a \qquad (2.6)$$

where K = σ_h/σ_v and Φ_a is the wall friction. The stress increase d6v can then be evaluated from $d\sigma_v A_b = \gamma g d_h$, + fφ dh, where γ is the density of the soil, φ is the perimeter of a cell, A_b is the area of a cell and g is acceleration due to gravity. This equation can be simplified to

$$d\sigma_v = [\ \gamma g + K\sigma_v tg\Phi_a / A_b\ ]dh \qquad (2.7)$$

The solution of this differential equation is:

$$\sigma_v = [\gamma g\, A_b / Ktg\Phi_a][e^{K\sigma v tg\Phi a / Ab}]dh \qquad (2.8)$$

The ultimate bearing capacity for cohesionless soils can be calculated from the general bearing capacity equation :

$$q_c = 0.6B\gamma gN_\gamma + q_o N_q \qquad (2.9)$$

where N_γ, and N_q are bearing capacity factors, B is the total width of the foundation grid, γ is the density of the soil and q_o is the overburden pressure at the foundation level. The bearing capacity factors N_γ, and N_q which depend on the angle of internal friction Φ are approximately equal to 20 at $\Phi = 30°$. The value of N_γ, and N_q increases rapidly with increasing Φ.

The transition from penetration failure to soil failure is independent of the size of the grid and of the size of the individual cells. It is only affected by the number of rows of cells (n) and by the angle of internal friction of the soil. Normally the bearing capacity of the grid foundation is governed by the penetration resistance except when the height of the cells (H) is relatively large in comparison with the width (L).

2.6.2 Cohesive Soils

Failure of a grid mat unit in clay can be caused by two different mechanisms. The first failure mode, penetration failure, governs when the height of the cells is reletively small in comparison with the circumference of the individual cells. The second failure mode, bearing capacity failure, governs when the height of the cells is relatively large. Then the friction or the adhesion of the soil along the vertical plates is sufficient to prevent the extrusion of the soil through the cells.

On the cohesive soil the ultimate bearing capacity of the grid (Q_{ult}) at penetration failure is dependent on the total surface are (A_m) of the individual cells in contact with the soil and on the adhesion c_a between the clay and the cell walls.

$$Q_{ult} = c_a A_m \qquad (2.10)$$

The adhesion ca is dependent on the undrained shear strength cu of the soil and on material of the grids. Experience from load tests with steel piles indicates that ca can be 0.5 c_u when $c_u < 50$ kPa and as low as 10 kPa when $c_u > 50$ kPa.

Failure by exceeding the bearing capacity of the soil occur when the cells are relatively high in comparison to the width. The ultimate bearing capacity of a square, triangular or circular grid unit can be calculated from :

$$Q_{ult} = (7.5\ c_u + q_o)\ A_b \qquad (2.11)$$

Where qo is the total overburden pressure at the bottom of the grid and A_b is the total bottom area. The adhesion along the outside perimeter of the foundation elements has been neglected in the derivation of this equation since the adhesion generally is relatively small.

Miki, (1996) explain, if reinforcing materials and a load of the earth cover are applied to soft ground with a high water content, the bearing capacity is expressed as sum of four components that is:
Bearing capacity of conventional ground:

$$q_1 = cN_c \qquad (2.12)$$

Bearing capacity resulting from tensile force generated et both end of the reinforcing material :

$$q_2 = 2T \sin \theta/B \qquad (2.13)$$

Effect of reinforcing material pressing down the ground:

$$q_3 = T\,[Nq/r] \tag{2.14}$$

Embedment effect resulting from settlement and rising:

$$q_4 = r_t D_f \tag{2.15}$$

Where c: denotes the cohesion of soft ground, N_c, N_q : the bearing capacity factor. T :the tensile force of the reinforced material, θ the angle formed by the reinforcing material and the horizontal surface at the end of the load, B : the load width, r: the radius of the deformed shape of the ground near the load when the shape is considered as circular, r_t : The weight per unit volume and D_f : theamound of settlement of the soft ground.

Thus, the ultimate bearing capacity is calculated as follows :

$$q_d = q_1 + q_2 + q_3 + q_4$$
$$= cN_c + 2T\sin\theta/B + T\,N_q/r + r_t D_f \tag{2.16}$$

2.7 Settlement

Any structure built on soil is subject to settlement. Some settlement is inevitable and, depending on the situation, some settlements are tolerable. When building structures on top of soils, one needs to have some knowledge of how settlement occurs and predict how much and how fast settlement will occur in a given situation. Important factors that influence settlement:

1. Soil Permeability
2. Soil Drainage

3. Load to be placed on the soil
4. History of loads placed upon the soil
5. Water Table

Settlement is caused both by soil compression and lateral yielding (movement of soil in the lateral direction) of the soils located under the loaded area. Cohesive soils usually settle from compression while cohesionless soils often settle from lateral yielding - however, both factors may play a role. Some other less common causes of settlement include dynamic forces, changes in the groundwater table, adjacent excavations, etc. Compressive deformation generally results from a reduction in the void volume, accompanied by the rearrangement of soil grains. The reduction in void volume and rearrangement of soil grains is a function of time. How these deformations develop with time depends on the type of soil and the strength of the externally applied load (or pressure). In soils of high permeability (e.g. coarse-grained soils), this process requires a short time interval for completion, and almost all settlement occurs by the time construction is complete. In low permeable soils (e.g. fine-grained soils) the process occurs very slowly. Thus, settlement takes place slowly and continues over a long period of time. In essence, a graph of the void ratio as a function of time for several different applied loads, provides an enormous amount of information about the settlement characteristics of a soil.

2.7.1 Calculating the Settlement

In calculating the final settlement due to to consolidation, use the appropriate equation as follow:

$$S = [e_o\text{-}e/1+e_o]H \quad (2.17)$$

$$S = m_v \Delta p H \quad (2.18)$$

$$S = H\,[C_c/1+e_o]\,log[P_o+\Delta P / P_o\,] \quad (2.19)$$

Where,

S : Settlement due to consolidation

H : target thickness of layer of soil

e_o : Initial void ratio

e : target void ratio

m_v : volume change rate

ΔP : load change

C_c : compression index

P_o : yield consolidation load

2.7.2 Calculating the Loading Period

Assuming that one dimensional consolidation applies to the consolidation, calculate the degree of consolidation, which corresponds to the loading period and the time factor, using the following formula:

$$T = [H_d^2/c_v]T \quad (2.20)$$

$$U = [T^3/(T^3+0.5)]^{1/6} \quad (2.21)$$

Where,

t : loading period

H_d : drainage distance: in case of draining to both side : $H_d = H/2$

c_v : coefficient of consolidation

T : Time factor

U : degree of consolidation

We use the degree of consolidation in this formula similar to that Terzaghi's theoretical formula, because they are price and simplify the calculation. For reference, when $T_{70} = 0.403$, $T_{80} = 0.567$ and $T_{90} = 0.848$, then the formula give $U = 0.698$, 0.802 and 0.905, respectively.

2.7.3 Selecting the Drain material

Calculate the maximum drainage speed per 1 meter of drain width from drainage when the degree of consolidation is 10%, as follow:

$$v = [HL\varepsilon_{10}]t \quad (2.22)$$

Where,

v : maximum drainage speed

H : thickness of soil layer to be improved Covered by drains on each level

L : length of layer covered by the drains

ε_{10} : volume compression strain at 10% consolidation

t : loading period till the degree of consolidation of 10%

2.7.4 Calculating the Strength Increase

Calculate the increased strength of the improved soil using the following formula:

$$\Delta c = [cu/p] \,.\, U.\, \Delta P \quad (2.23)$$

Where,

Δc : increase strength

$[cu/p]$: strength ratio P

U : degree of consolidation

ΔP : load change

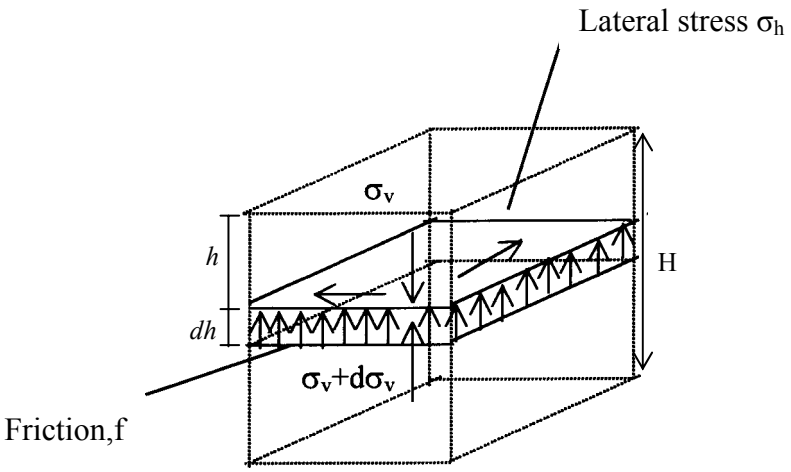

Figure 2.1: Stress distribution within a cell for rectangular

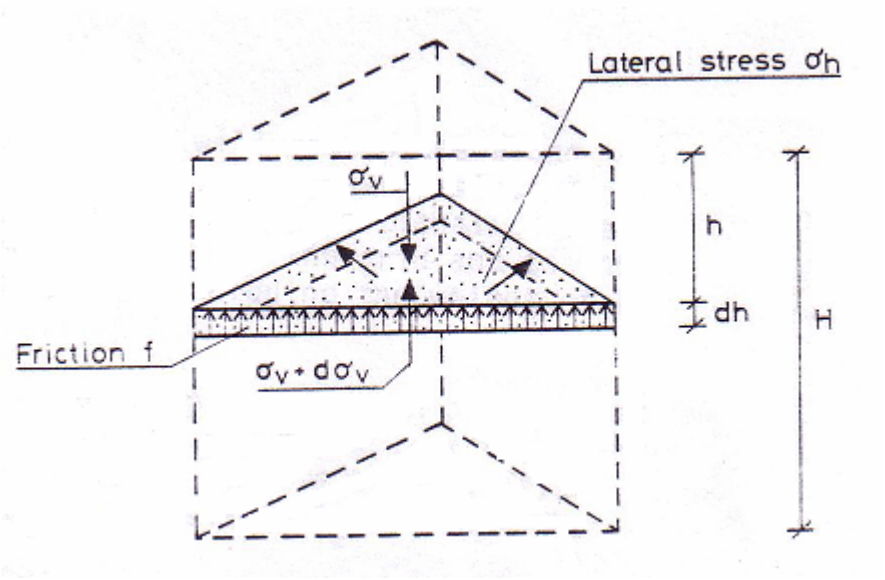

Figure 2.2: Stress distribution within a cell for triangular

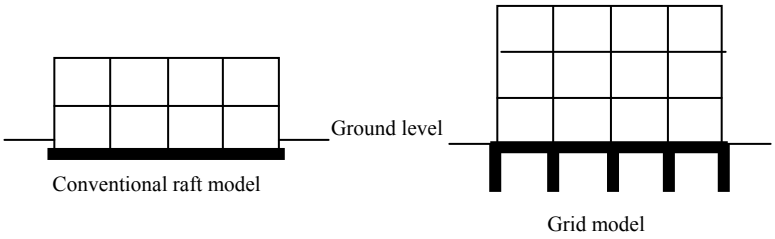

Figure 2.3 : Grid model

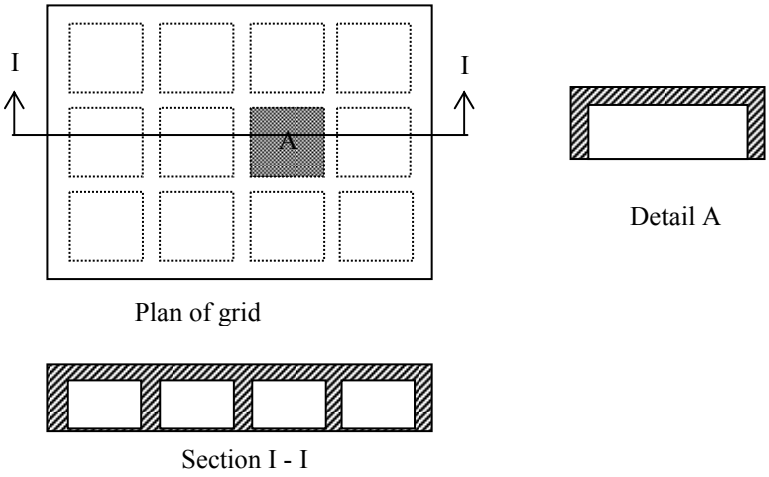

Figure 2.4 : Detail diagram of grid model

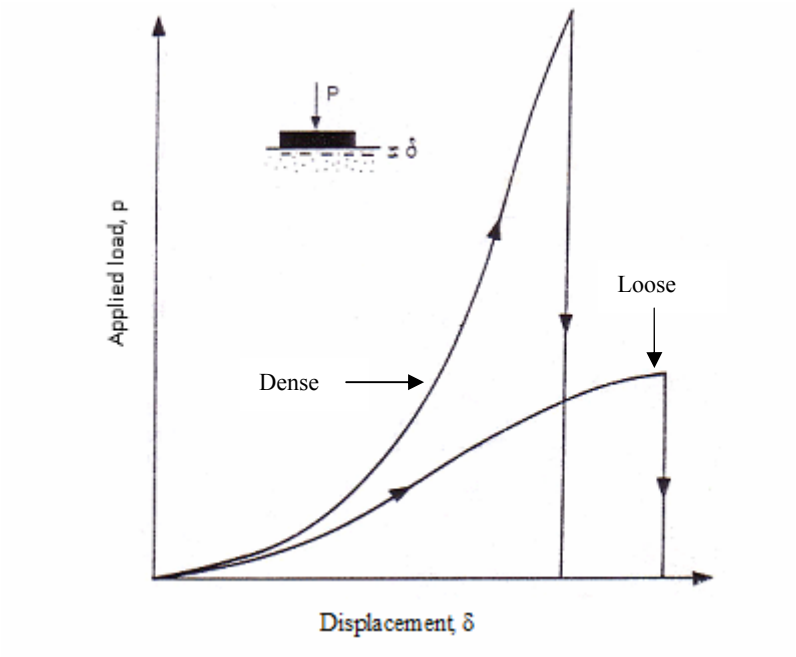

Figure 2.5 : Load-displacement relationships for grid placed at the surface

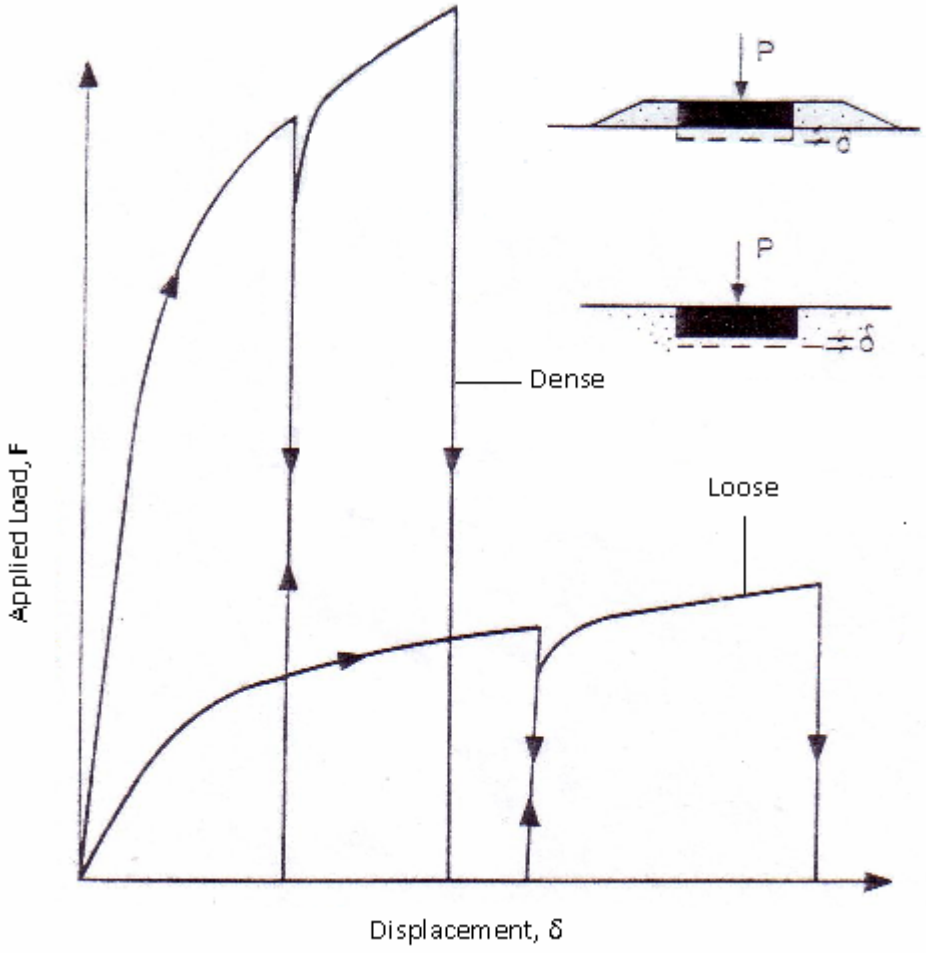

Figure 2.6 : Load-displacement relationships when fill has been placed around the grid or when the grid has been pushed into the under-lying soil

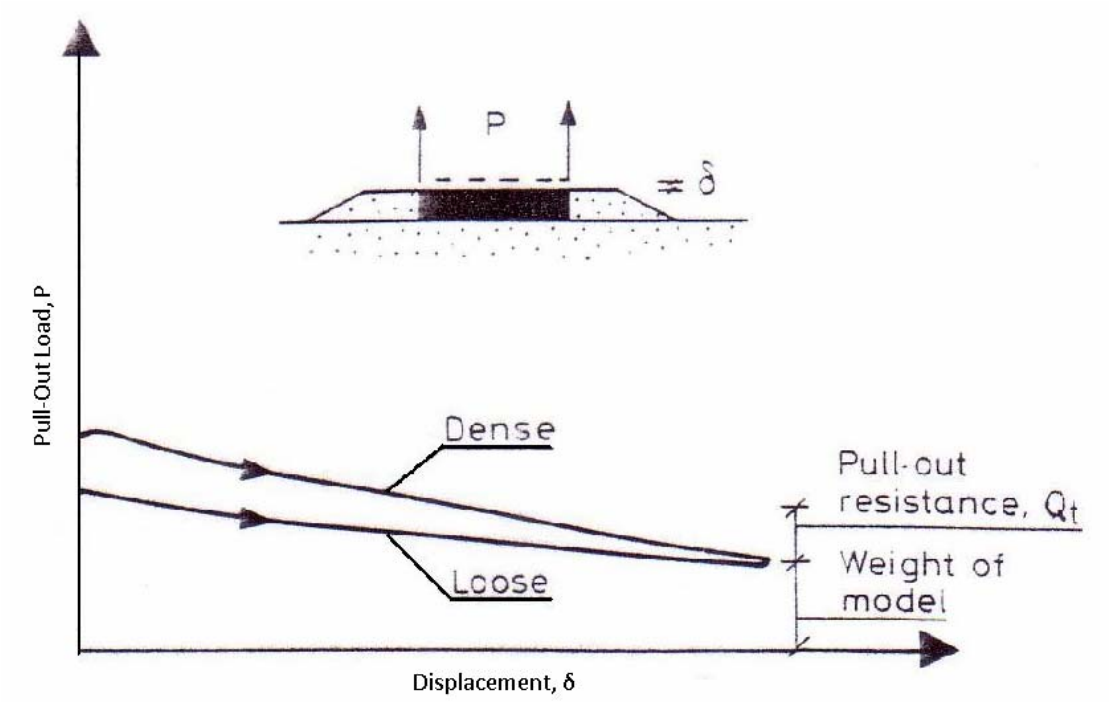

Figure 2.7 : Load-displacement relationships at pull-out tests after the grid has been pushed into the underlying soil.

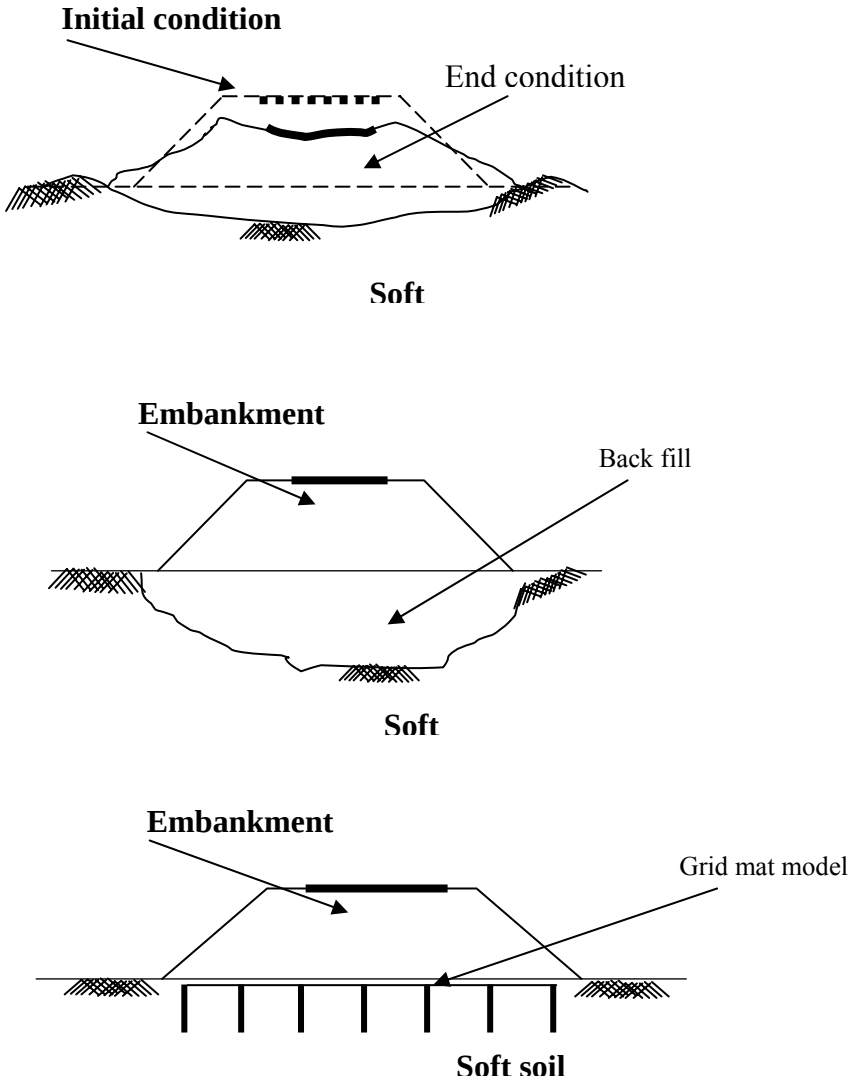

Figure 2.8 : Bearing capacity of soft soil

CHAPTER 3

RESEARCH METHODOLOGY

3.1 Introduction

This chapter will discuss the model testing of grid mat that were used in this experimental study. This study incorporated a laboratory test and evaluation the potential of grid mat to increasing the bearing capacity of subgrade soils. Laboratory test and analysis oriented to references, journals books and geotechnics standard. Experimental has been done in Geotecnical Lab, Fakulti Kejuruteraan Awam, UTM. The testing program includes the finding of the basic engineering characteristics of the materials used in the models tests, followed by the model test. Each model test consists of two stages : consolidation stage and loading test stage.

3.2 Outlines of Methodology

The overview of methodology procedures is shown in a shematic flow chart as in Figure 3.1. Basically, the methodology contains several steps. The study started with the identification of the problem area. The problem area is to identify the study

problem, scope of study, objective of study and significance of study.

Further step taken to continue this study is by conducting the literature review. Literature review was done to provide the background to the study to get an insight to researching techniques which has been employed in previous studies. It mainly relates to the characteristics of subgred soil whether the properties or the classification of subgred soil, bearing capacity of subgred soil and finally the method of testing the bearing capacity of subgred soil as for laboratory tests.

This study was based on the laboratory model tests. There are 3 model of grid mat is used in this test. There are diamond pattern, chevron pattern and square pattern. Each model test consists of two stages : consolidation stage and loading test stage. Figure 3.17 shows the example of the grid mat models. The soils samples were disturbed sample made of koalin powder mixed with appropriate percentage of water. The properties of the koalin powder were determined via physical and shear strength tests before the model tests were performed.

After conducting laboratory test, that is the bearing capacity test, the data obtained from the tests were analyzed and presented in the chart and graph form. The data were also analyzed to obtain the effect of grid mat pattern on bearing capacity.

Finally, a few conclusions can be withdrawn from the data analysis. In this part of study, the effect of grid mat pattern on bearing capacity test will be discussed. The results obtained from the data analysis and also form the chart and graph will be referred to make some conclusions based on the objectives of the study made earlier in the first chapter.

3.3 Laboratory Works

As we known, the grid method included foundation that always build from concrete plate purposes for transmit the column or wall loading to the ground. The grid method always used in soft ground that have the lower bearing capacity to prevent the settlement. The objective of literature study is to compile the finding soil reinforces and the application. To what extend the using of geogrid material to stabilize in the geotechnical engineering approaches

3.3.1 Field Work and Sampling

The study started with collection and preparation of soil sample.The purpose of the field works to collecting sample of soil will be use for testing processes and the application, the soils are disturbed sample made from the koalin powder mixed with certain percentage of water and determine of soil classification and engineering properties of soil. Figure 3.2 shows the example of koalin powder that used in this study. The soil sample used in this study were koalin powder, obtained from local supplier.

3.3.2 Soil Classification Test

The laboratory test for determination engineering characteristic of soil sample is needed to achieve the objective. The test of soft soil had been carried out according to BS 1377 (1990) and the list of the all test are shown in Table 3.1. The analysis of soil classification consist of specific gravity (SG), liquid limit (LL), plastic limit (PL), plastic index (PI), shrinkage limit (SL) and vane shear test (Cu).

3.3.2.1 Specific Gravity (SG)

The average mass per unit volume of the solid particles in soil samples, where the volume includes any sealed oids contained within solid particles is called specific gravity or particle density. The specific gravity was measured using density bottle (small pyknometer method) is followed BS 1377 : Part 2 : 1990 : 8.3 (Figure 3.3). About 30g oven dried soil at 105-110˚C were divided into three approximately and place each into a density bottle. The de-aired distilled water was added to each bottle and applied vacum to remove the air trapped. Then, the bottle transferred to constant-temperature bath until the bottle remains full. In order to calculate the S.G, the weigh of bottle with soil and the bottle with liquid were measured. The calculation of particle density or specific gravity is gien as following equation:

$$SG = \frac{(m_2-m_1)}{(m_4-m_1)-(m_3-m_2)}$$

where m_1 = mass of density bottle (g)

m_2 = mass of bottle + dry soil (g)

m_3 = mass of bottle + soil + water (g)

m_4 = mass of bottle + water only (g)

3.3.2.2 Atterberg limits

The atterberg limits of soil could provide a means of measuring and describing the plasticity range in numerical terms. The tests to measure the atterberg limit are carried out on the fraction of soil, which passes a 425 μm sieve. The atterberg limit consist of liquid limit, plastic limit and plastic index. The liquid limit (LL) is the moisture content at which soil go by from the plastic to the liquid state . whereas, the moisture content at which soil go by plastic conditions is called plastic limit. The liquid limit was measured by cone penetration method followed BS 1377 Part 2 :

1990. 4.3 (Figure 3.4). About 300gm of the prepared soils paste were placed on the glass plate before placing into the cup. The liquid limit is calculated at the cone penetration of 20mm.

Plastic limit (PL) was determined by followed BS 1377 Part 2 : 1990. 5.3. The test carried out on soil prepared by the wet preparation. About 20gm of the prepared soil paste were spread on the glass mixing plate. The soil mix occasionally, well pressed and shaped into a ball then formed into a thread. Mould the ball between the fingers. Using a steady pressure, roll the thread to about 3mm until the cracks begin to appear on the surface. For the calulation, measured the moisture content of soil thread, and the differ less than 0.5% moisture content is reported as the plastic limit.

The Plasticity Index (PI) is the numerical difference between liquid limit and plastic limit. Plasticity inde is determined by followed BS 1377 Part 2 : 1990. 5.4. Therefore, the plasticity index of the soil is given by the follow equation :

$$PI = LL - PL$$

3.3.2.3 Shrinkage Test

Shrinkage limit (SL) is the moisture content at which a soil on being dried stop to shrink. Shrinkage ratio is the ratio of the change in volume to the corresponding change in moisture content above the shrinkage limit. Shrinkage limit test – alternative method are given in BS 1377 : Part 2 1990. 6.4 and ASTM D427. About 30gm soil passing the 425μm sieve were mixed with distilled water to make into a readily workable paste. The moisture content should be greater than the liquid limit or to give about 25-28mm penetration of the cone penetrometer. The soil were place in a shrinkage dish, leave to air dry for a few hours, or overnight then place in

oven at 105-110˚C. The internal volume of wet soil and the dried soil were measured with mercury. The shrinkage limit can then be calculated from the equation :

$$SL = \frac{w_1 (V_1 - V_d) \times 100\%}{(m_d)}$$

where, w_1 = moisture conent of the initial wet soil

V_1 = volume of wet soil pat (ml)

V_d = volume of dry soil pat (ml)

m_d = mass of dry soil (g)

3.3.2.4 Vane Shear Test

The vane shear test is used to to find shear strength of a given soil sample. The structural strength of soil is basically a problem of shear strength. Vane shear test is a useful method of measuring the shear strength of soft soil. It is a cheaper and quicker method. The test can also be conducted in the laboratory. The laboratory vane shear test for the measurement of shear strength of cohesive soils, is useful for soils of low shear strength (less than 0.3 kg/cm^2) for which triaxial or unconfined tests can not be performed. The test gives the undrained strength of the soil. The undisturbed and remoulded strength obtained are useful for evaluating the sensitivity of soil. Prepare three specimens of the soil sample of dimensions of at least 37.5 mm diameter and 75 mm length in specimen. Mount the specimen container with the specimen on the base of the vane shear apparatus. If the specimen container is closed at one end, it should be provided with a hole of about 1 mm diameter at the bottom. Gently lower the shear vanes into the specimen to their full length without disturbing the soil specimen. The top of the vanes should be atleast 12 mm below the top of the specimen. Note the readings of the angle of twist. Rotate the vanes at an uniform rate say 0.1^o/s by suitable operating the torque application handle until the specimen fails. Figure 3.5 shows the example of the shear vanes with their specimen container.

3.3.3 Model Testing Equipment

Experimental setup consists of a soil container, grid mat models and loading equipment. The vertical load was applied to the grid mat model using loading equipment that provided a constant rate,of vertical displacement. The loading equipment is compression testing machine with maximum capacity 1000 kN. A load cell and a linear variable displacement transducers (LVDT) were used for measuring load grid displacement, to keep in existenceb of coarseness surface of this models so the models surface are layered by sand paper.

3.3.3.1 Models of Grid Mat

The model grid mat is rectangular and triangular. The models were fabricated of fiber glass and the bearing area was covered by sandpaper to provide a rough base. In this study, 3 models are build with different shape and there are rectangular pattern chevron pattern and diamond pattern. The material of the model made from steel plates measuring 175 mm length x 150 mm width x 50 mm height. Figure 3.18 (a), (b), (c) and (d), shows a picture of the grid mat models, and the dimension of grid mat model has been presented in Table 3.2.

3.3.3.2 Soil Box Container

The soil box container is a box plexiglass with thickness 12.5 mm have 620 mm long, 620 wide and height of 1000 mm. Four holes in opposite sides were drilled 10 mm from the bottom of the box, and four valves were installed in these holes to control the drainage during the consolidation stage and grid mat model test stage. The

illustrative of soil box container shown in Figure 3.6 and the dimension of soil box container has been presented in Figure 3.7.

3.3.3.3 PVC Plate

A PVC plate with dimension of 60cm x 60cm and 0.1cm height were use in the consolidation process. The PVC plate used as platform for steel frame. Holes in the plate were drilled 10mm to control the drainage during the consolidation stage. The illustrative of PVC plate shown in Figure 3.8 and the dimension of PVC plate has been presented in Figure 3.9.

3.3.3.4 Steel Frame

A steel frame with dimension of 60cm x 60cm were used in consolidation process as connection between loading plate and PVC plate during the consolidation process. The illustrative of steel frame shown in Figure 3.10 and the dimension of grid mat model has been presented in Figure 3.11.

3.3.3.5 Loading Plate

A plate with dimension of 59.5 cm x 59.5 cm and 1.5 cm height were use in the consolidation process. The plate used to make sure that the consolidation occurs even before the loading take place. The loading plate reinforced with steel frame at edge to prevent changes during the consolidation process.

3.3.3.6 Load Cell

The load cell with a capacity of 300kgf was used to estimate the loads that push the grid mat during the loading process. The CLP-300 kA model load cell is made by Tokyo Sokki Konkyujo Co. Ltd. and has a sensitivity of 1.5 V/V and coefficients of 0.980. Before the cell can be use it's has to be calibrated to check whether the cell is accurate or not. The load cell are attach to the load join that are made from steel plate with 4 screw hole and 10mm height.

For consolidation of marine clay and clay sand, BLB-5Tb model with capacity of 5000kgf made by Kyowa Electronic Instrument Co. Ltd. were used to monitor the pressure that given to the foundation soil. This cell has coefficient of 1.25 and picture is illustrate in Figure 3.12.

3.3.3.7 Linear Variable Displacement Transducers (LVDT)

To record settlements that occur during the loading stage the used of LVDT is essential to predict the bearing capacity of the grid mat. The LVDT that use in the experiment are from Tokyo Sokki Konkyujo Co. Ltd. with CDD-100 model with a capacity of 100 mm settlement. Before it can be use the LVDT has to be calibrating to closest value of 1.00. For loading stage the LVDT are put in two positions so that the average value can be use as the settlement value. This because there will be error during the reading when one of the end settle differently. The LVDT are fix to frame by magnetic so that there are no error when taking data. The picture of LVDT are shown in Figure 3.13.

3.3.3.8 Portable Data Logger

Data from load cell and LVDT are recorded to data logger during the loading process. This data collection process is to record the value of settlement and the pressure that push the grid mat and foundation soil. This data logger is production of Tokyo Sokki Konkyujo Co. Ltd. with TDS-310-85 model. The Picture of portable data logger are shown in Figure 3.14.

3.3.3.9 Hydraulic Jet

Hydraulic Jet use to giving the load during the consolidation test on soft soil for determination the nearing capacity of grid mat model. The hydraulic jet that having used is model 35100 C with 35,000 kgf capacity. The load that produced from jet hydraulic is determined through the load cell that connected with portable data logger.

3.3.3.10 Motor Hydraulics Control

During the testing, 1,000 kN capacity of motor hydraulic control will used to carry out the loading test. Motor hydraulics control consists hydraulics gear box model TK-B, type 70, electric motor fram 2802-1 and electronic panel control model Toshiba, VF-S.7.200V-0.75 KW. The function of Hydraulic gear box and electric motor is to moving the load cell, while the electronic panel control is function to control the velocity of loading. Figure 3.15 shows the picture of motor hydraulics control.

3.3.4 Experimental Setup

The experimental study started with the identification of engineering characteristics of soft soil sample. Further step taken to continue this research is by conducting the preparation of soft soil sample and placement of grid mat models.

3.3.4.1 Preparation of Soft Soil Sample

The samples used in the study were made of koalin powder. The samples were prepared by mixing the koalin powder with 49% of water. The water percentage used for the sample preparation was determined by the plastic limit test. The plastic limit values of the koalin powder were in the range of 47% to 57%. Figure 3.16 shows the mixer machine used in this research. After the soft soil mixed with mixer machine about 20 minute, the soft soil paste will put in 4 soil box container using scoop untill the soil depth achieved 85cm. Then the sample maked flat for placement the grid mat models.

3.3.4.2 Placement of Grid Mat Model

After the preparation process had been completed, the grid mat model were placed on the top of the soil sample in soil box container. The picture of 4 type of models are shown in Figure 3.19. The grid mat model were placed with pressdown the model untill the model enter fully in the soft soil sample. Then, the plastic and pvc plate were placed on the top of the sample for act as platform of steel frame. For make easily the compaction process of soft soil during the consolidation test, steel frame is used as connection between loading plate and pvc plate. The consolidation test

conducted using loading frame and the test will take about 1 day to give the highest strength of soil sample before loading test.

3.5 Experimental Procedure

The testing program includes the finding of the grid mat that will give the highest bearing capacity. Each model tests consisted of two stages namely the consolidation stage and loading stage .

3.5.1 Consolidation Stage

In the consolidation stage, 2 cm thick poorly graded sand was placed at the bottom of the box model to serve as a drainage layer. A geotextile layer was then placed on top of the sand layer as a separator. Oven dried clay soil was mixed thoroughly with certain amount of water to achieve a moisture content of 32%. It was then placed in the box. The plate, measuring 600 mm x 600 mm and 15 mm thick, was placed on top of soil layer. To speed up the consolidation process, 5mm diameter holes were drilled on the loading plate, so that the soil layer would be doubly drained. Sheet filter were placed along the sides of the box, and between the soil and the loading plate, to accelerate the consolidation process.

The drainage valve was opened and a first load of 20 kPa was applied using a special loading frame. Soil deformation was monitored where two dial gauges connected to the loading plate, until the plot of settlement against the square root of time became nearly horizontal measured settlements reading as shown in Figure 3.20. The second load of 40 kPa was then applied to further the consolidation process. The

second layer has increase to 18cm height. The soil surface is flattened and the ribs are placed horizontally. After the loading plate are placed on the soil surface with the ribs and then the last load of 80 kPa was applied. The consolidation was stop after the 60% of the consolidation are achieved. After the consolidation was completed, the foundation model was then placed on the surface and at the centre of the soil in the box model.

Thereafter, the two valves at the bottom of the soil box were closed and the specified loading rate was set. Loads were then applied to the raft foundation through hydraulic jack, controlled by electric motor. The load applied to the raft model was measured by load cell while the displacement was measure by two LVDT where all of them were connected to a portable data logger.

Before the last load increment applied, the grids model was held vertically in place at the center of the box above third layers. The consolidation process was performed in a special loading frame using the lever type arrangement with a lever arm ratio of 1 : 10. The settlement of the soil layer was measured by means of two dial gauges connected to the loading plate on the top of the soil layer.

3.5.2 Loading Test Stage

After the consolidation of the soil had been completed, the consolidation load was removed and the soil box was carefully removed from the consolidation frame and mounted in the compression testing machine as shown in Figure 3.21. Thereafter the four valves at the bottom of the soil box were closed an specified loading rate was set as shown in Figure 3.22. The model of the grid was tested under five different loading rates, namely, 1 mm/min, 0.5 mm/min, 0.05 mm/min; and 0.01 mm/min. The

load applied to the model of grid was measured by load cell and the grid displacement was measured by LVDT.

The ultimate load, which is represented by dotted line, was defined at the point where the slope of the load-settlement curve first reaches a steady minimum value (Vesic, 1963, Hanna and Rahman, 1990, and Oda and Win, 1990). This concept was employed fror all models tested in the present investigation for the purpose of comparison and revealed a unique value for the ultimate load for each load-settlement curve. The vertical load was applied to the grid model using loading equipment, at a constant rate of vertical displacement. The compression machine with maximum capacity of 1,000 kN was connected to a portable data logger. Loads were applied to the grid foundation models through hydraulic jack, controlled by an electric motor. Figure 3.23 shows the effect of loading on soft soil after the loading test.

Table 3.1 : List of soil classification test

No.	Test
1.	Specific gravity (SG)
2.	Atterberg limit • Liquid limit (LL) • Plastic limit (PL) • Plastic index (PI)
3.	Shrinkage limit (SL)
4.	Vane shear test (Cu).

Table 3.2 : Dimension of grid mat models

No.	Pattern	Length (L) (cm)	Width (B) (cm)	Height (H) (cm)
1.	Chevron	17.5	15.0	5.0
2.	Diamond	17.5	15.0	5.0
3.	Square	17.5	15.0	5.0

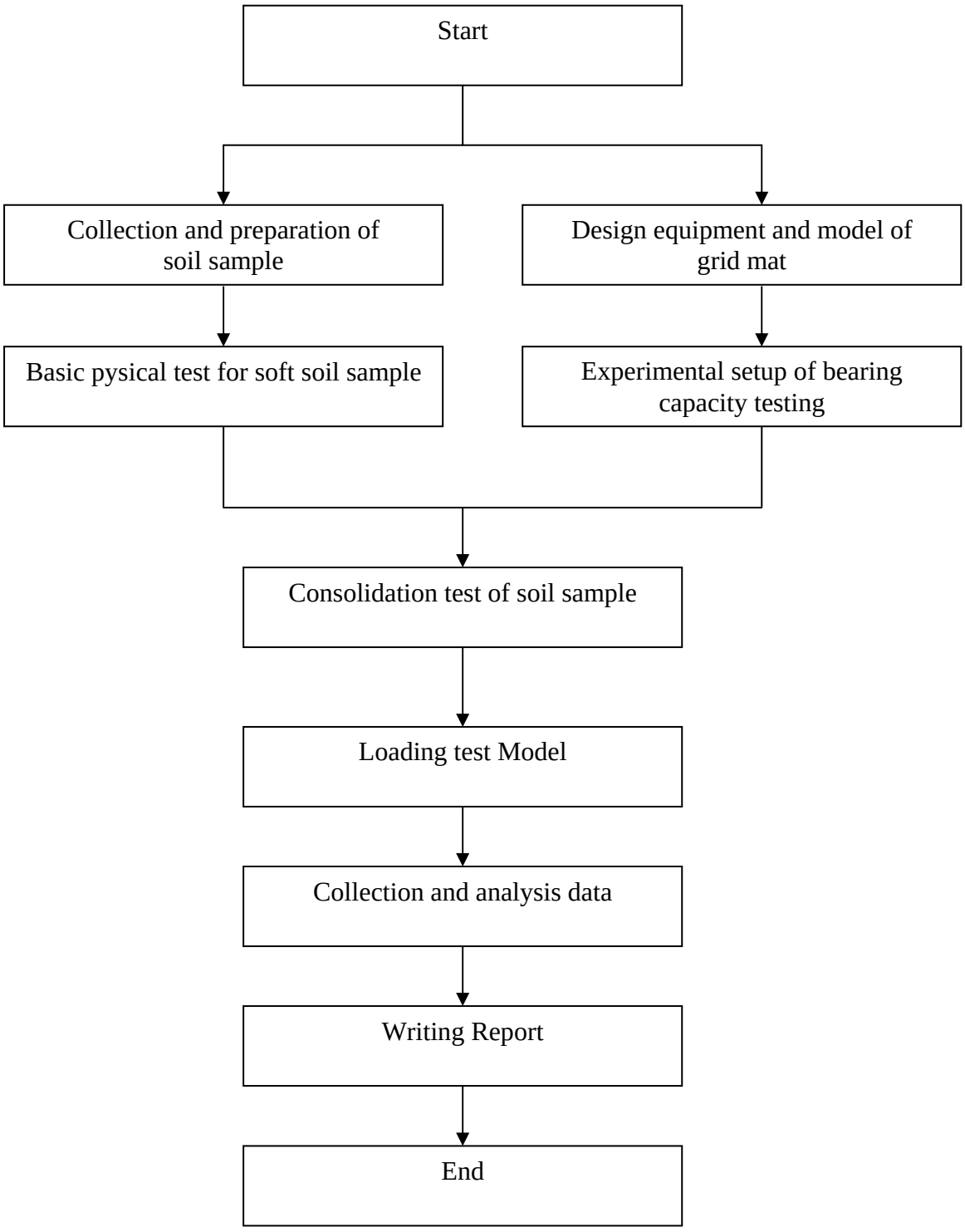

Figure 3.1: Flow chart of experiment

(a)

(b)

Figure 3.2 : Example of Koalin Powder

Figure 3.3 : Specific Gravity Test

Figure 3.4 : Penetration cone

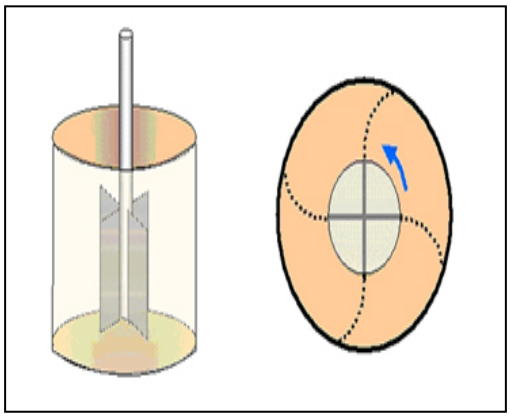

Figure 3.5 : Example of the shear vanes with their specimen container

Figure 3.6 : (a) Front view (b) Side view of soil box container

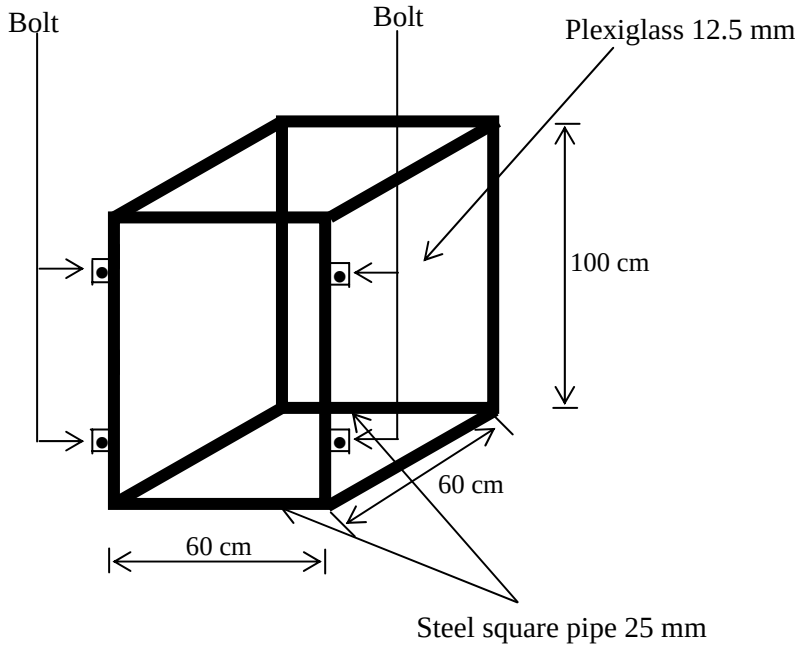

Figure 3.7 : Dimension Soil box container

Figure 3.8 : PVC Plate

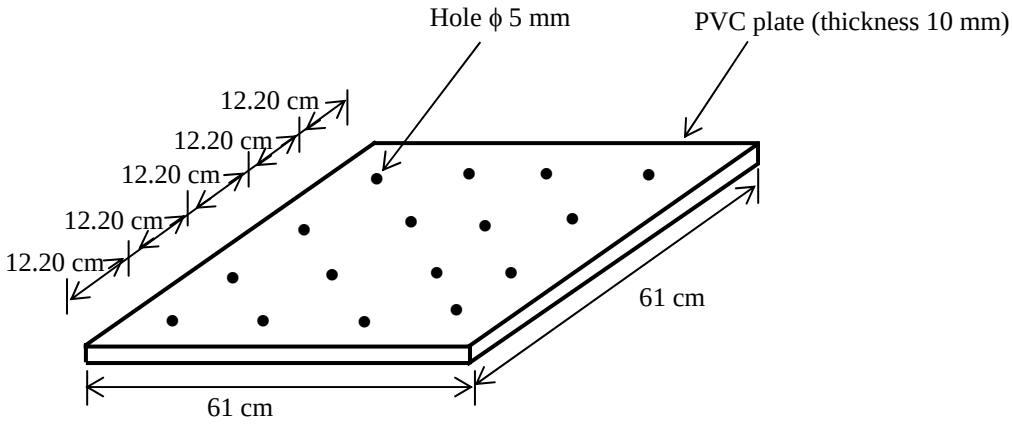

Figure 3.9: Dimension of PVC Plate

Figure 3.10 : Steel Frame

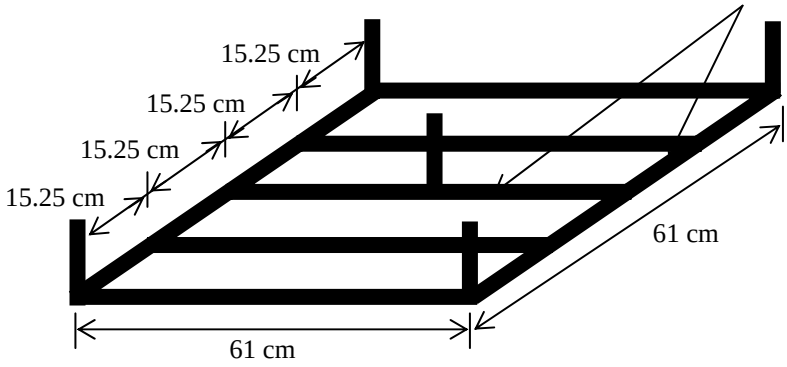

Figure 3.11 : Dimension of Steel frame

Figure 3.12 : Picture of load cell

Figure 3.13 : Linear Variable Displacement Transducers (LVDT)

Figure 3.14 : Portable data logger

Figure 3.15 : Loading Motor

Figure 3.16 : Mixer Machine

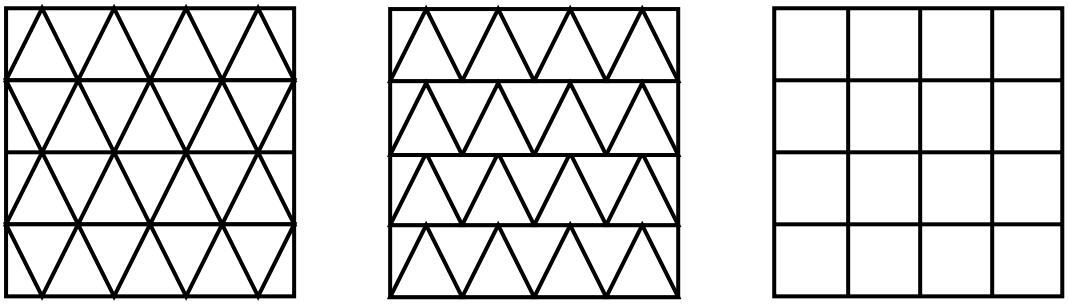

a) Diamond Pattern b) Chevron Pattern c) Square Pattern

Figure 3.17 : Example of Grid Mat Models

(a) Plywood (Load Connection)

(b) Square Pattern

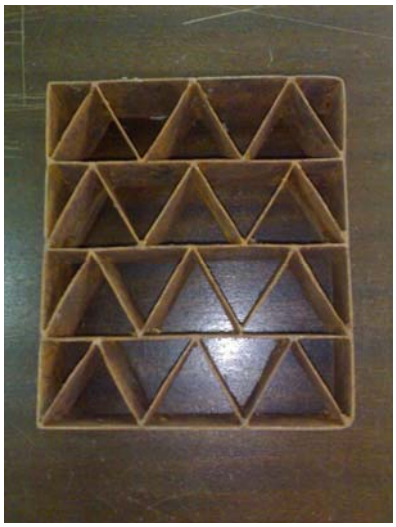

(c) Chevron Pattern

(d) Diamond Pattern

Figure 3.18 : Picture of Grid Mat Models

(a) Square Pattern

(b) Diamond Pattern

Figure 3.19 Placement of grid mat models

Figure 3.20 : Consolidation Test

Figure 3.21 : Loading Test Frame

(a)

(b)

(c)

Figure 3.22 : During Loading Test

(a)

(b)

(c)

Figure 3.23 : After Loading Test

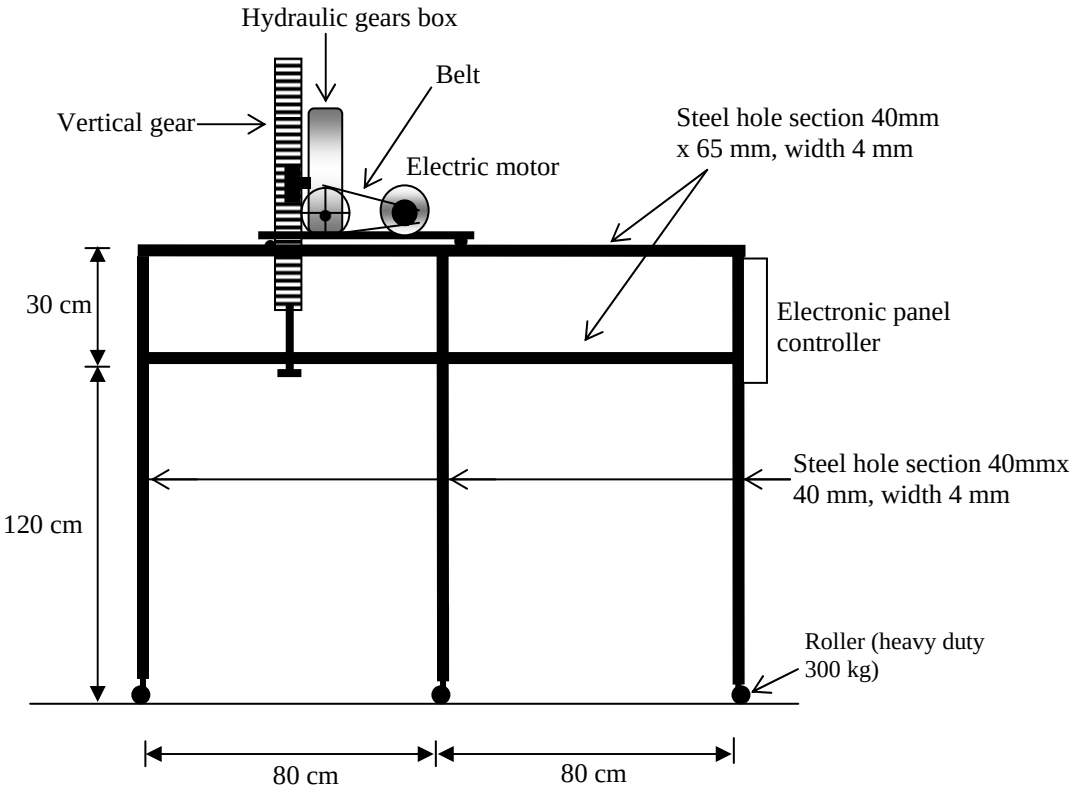

(a) Front view

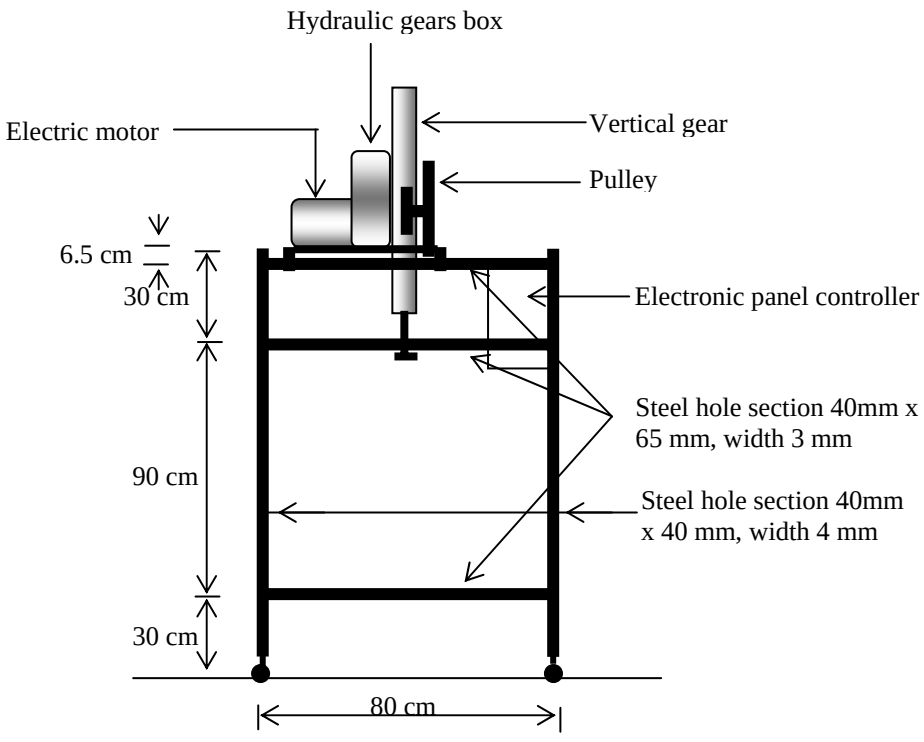

(b) Side view

Figure 3.24 : Dimension of Loading Frame

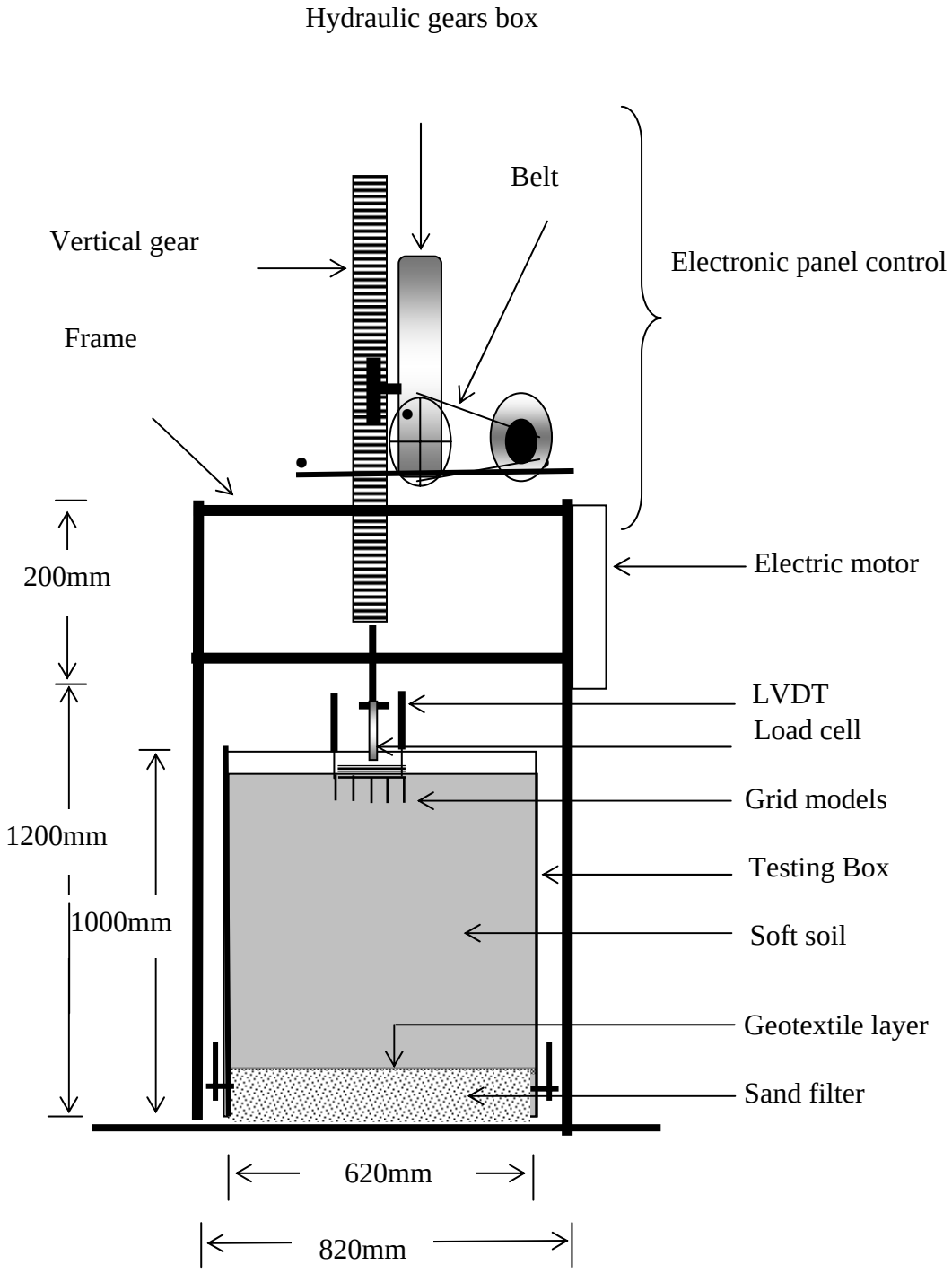

Figure 3.25 : Schematic diagram of laboratory test setup

CHAPTER 4

LABORATORY AND EXPERIMENTAL RESULTS

4.1 Introduction

This chapter discusses about the analysis and the results of the geotechnical properties of the soil samples and the experimental test model. The geotechnical properties of the soil samples vary although they come from same site, due to the complexity of the materials. Standard systems of testing for soil properties and classification are needed in order to eliminate human errors. British Standard Methods of test for soil for civil engineering purposes (BS) and American Society for Testing and Materials (ASTM) can be used depending upon the suitability and availability of equipment. The results obtained from the laboratory test conducted for the reinforced soil model are also discussed in this chapter. The test data were collected and presented in the tabular and graphical forms. The maximum values of the bearing capacity load and vertical displacement for each model are discussed.

4.2 Laboratory Results on Properties of Kaolin

The soil sample used in this study is produced from homogeneous soil called Kaolin obtained from a local supplier and is a commercial soil used mainly in the kaolin industry. Table 4.1 shows the typical specifications of refined Kaolin as given by the supplier. The laboratory tests for physical and strength properties in this study consist of specific gravity (SG), liquid limit (LL), plastic limit (PL), Plastic Index (PI), shrinkage limit (SL) and vane shear test (c_u).

Table 4.1 : Typical specification of refined Kaolin

Parameter	Value
Grade	L/2
Physical Properties:	
Moisture content	Below 3%
Viscosity (30% Solution)	40-200cp
pH (30% Solution)	5.0-6.0
Brightness	75-795GE
Average Particle size	9-12µ
Distribution 2µ	5-15%
10µ	50-65%
Chemical Composition:	
Alumina (Al_2O_3)	20-30%
Silica (SiO_3)	55-65%
Iron Oxide (Fe_2O_3)	Below 1.5%
Potash (K_2O)	Below 2.0%
Magnesia (MgO)	Below 1.0%
Ignition Loss @ 850ºC for 2 hours	8-10%

4.2.1 Specific Gravity (SG)

Table 4.2 shows the results of the specific gravity for the kaolin specimens. The average value of the specific gravity of the kaolin sample for this study is about 2.52. The specific gravity of the kaolin sample is below than the specific gravity of typical soil (about 2.7), is due the existence of organic matter in the kaolin.

Table 4.2 : Specific gravity of Kaolin

No. Pyknometer	1443	1799	1413	1412
Weight of pyknometer (W_1) g	35.69	31.69	24.47	35.89
Weight of pyknometer + sample (W_2) g	42.66	35.77	30.56	41.30
Weight of pyknometer + sample + water (W_3) g	90.50	82.17	80.04	89.34
Weight of pyknometer + water (W_4) g	86.24	79.74	76.32	86.11
Weight of sample (W_2 - W_1) g	6.97	4.08	6.09	5.41
Weight of water volume equivalent with soil (W_4-W_1)-(W_3-W_2)g	2.71	1.65	2.37	2.18
Specific gravity, $G_S = \frac{W_2-W_1}{(W_4-W_1)-(W_3-W_2)}$	2.572	2.473	2.570	2.482
Average of specific gravity, G_S	**2.52**			

4.2.2 Liquid Limit (LL)

Table 4.3 shows the results of the liquid limit tests for the kaolin sample. Figure 4.1 shows the graphical construction for the determination of the liquid limit value based on the graph of cone penetration versus moisture content. The liquid limit was obtained at the intersection of the vertical line and the cone penetration of 20 mm. Therefore the value of the liquid limit is estimated as 49%.

Table 4.3 : Liquid limit of Kaolin

No. of testing	1	2	3	4
Initial Reading (mm)	0	0	0	0
Final Reading (mm)	18.733	23.033	24.200	30.500
Cone Penetration	18.733	23.033	24.200	30.500
No. of container	84 B	113 B	102 B	119 B
Weight of container (g)	9.737	9.453	10.048	9.389
Weight of container + wet sample (g)	17.510	20.267	24.177	22.646
Weight of container + dry sample (g)	15.000	16.624	19.289	17.861
Weight of moisture (g) M_w	2.510	3.643	4.888	4.785
Weight of dry sample (g) M_s	5.263	7.171	9.241	8.472
Moisture content, (%) M_w/M_s	47.691	50.802	52.895	56.480

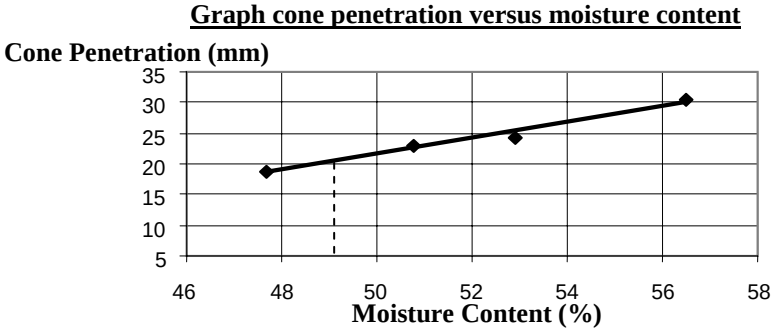

Figure 4.1 : Graph of cone penetration versus moisture content

4.2.3 Plastic Limit (PL)

Table 4.4 shows the result of the plastic limit test for the kaolin sample. The plastic limit for kaolin sample obtained in this study was 32%. The value was determined from an average value of moisture content from specimens which started to crack at rolled diameters of 3 mm.

Table 4.4 : Plastic limit of Kaolin

No. of testing	1	2	3	4
No. of container	97 B	57 B	69 B	106 A
Weight of container (g)	6.817	6.724	6.606	6.822
Weight of container + wet sample (g)	9.600	10.381	10.644	11.864
Weight of container + dry sample (g)	8.841	9.520	9.777	10.690
Weight of moisture content (g) M_w	0.759	0.861	0.867	1.174
Weight of dry sample (g) M_s	2.024	2.796	3.171	3.868
Moisture content (%) M_w/M_s	37.500	30.794	27.342	30.352
Plastic limit (%)	**32.00**			

4.2.4 Plastic Index (PI)

Plasticity index is the numerical difference between liquid limit and plastic limit. Therefore, the plasticity index of the kaolin is given by the following equation :

$$PI = LL - PL$$
$$= 49\% - 32\%$$
$$= \mathbf{\underline{17\%}}$$

4.2.5 Shrinkage Limit (SL)

Linear shrinkage (L_s) is the change in length of a bar sample of soil when dried from about its liquid limit. It is expressed as a percentage of the initial length. The calculation of the linear shrinkage as a percentage of the original length of the specimen is from the following equation, which is L_p = original length (140 mm for the standard mould) and L_o = length of the dry specimen.

$$L_s = [1 - (L_p/L_o)] \times 100\%$$
$$= [1 - (140/157)] \times 100\%$$
$$= \mathbf{\underline{11\%}}$$

4.2.6 Vane Shear Test

The vane shear test in the study was conducted using Geinor vane shear model. The instrument consists of 3 set of vanes, i.e, large, intermediate and small sizes with their coefficients of l/d of 2, 1 and 0.5 respectively. Table 4.5 shows the result of the testing. From the table 4.5, the average cohesion value of the kaolin, c_u =12.0kPa. The c_u value is obtained by substracting the friction of the rod from the shear strength value and then multiplying by the coefficient l/d.

Table 4.5 : Vane shear test results for Koalin

No.of vane	Diameter, d (cm)	Length, l (cm)	Coefficient (l/d)	No. of testing	Friction of rod (kPa)	Shear reading (kPa)	c_u (kPa)
1	2.0	4.0	2.0	1	1	7.0	12.00
				2	1	6.5	11.00
2	2.0	2.0	1.0	1	1	12.5	11.50
				2	1	12.0	11.00
3	2.0	1.0	0.5	1	1	25.5	12.25
				2	1	25.0	12.00

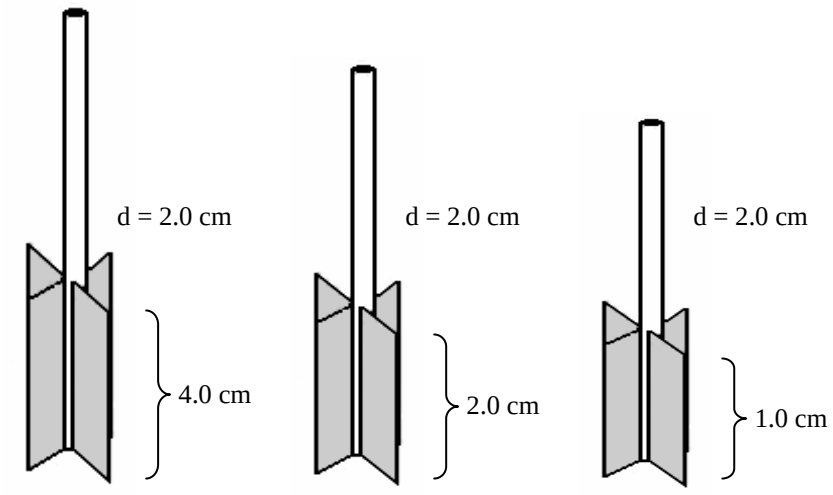

Figure 4.2 : Schematic Diagram of Dimension of vanes used in the laboratory test

4.2.7 Summary of Laboratory Test Results

Table 4.6 shows the summary of the all laboratory testing results for the kaolin sample used in this study.

Table 4.6 : Summary of result for all tests

Testing	Kaolin
Atterberg Limit	
Liquid Limit (%)	49.0%
Plastic Limit (%)	32.0%
Plasticity Index (%)	17.0%
Shrinkage Limit (%)	11%
Specific Gravity, G_S	2.524
Vane Shear Test – c_u (kN/m^2)	12 kN/m^2

4.3 Result on Effects of Reinforced Grid Mat on Settlement and Bearing Capacity

In the study, the data for the settlement measurement were obtained using the Linear Variable Displacement Transducer (LVDT). Beside a control model (non-reinforced), there were three models for the reinforced soil models, i.e, diamond pattern, chevron pattern and square pattern. The average data from 2 LVDT were estimated as the settlement values for plotting the graph. The results of the settlement test of soft soil reinforced by using grid mat method on various pattern in this study are illustrated in Figures 4.3, 4.4, 4.5, and 4.6. Figure 4.7 shows the graph of force in Newton versus settlement in millimeter for all model tests.

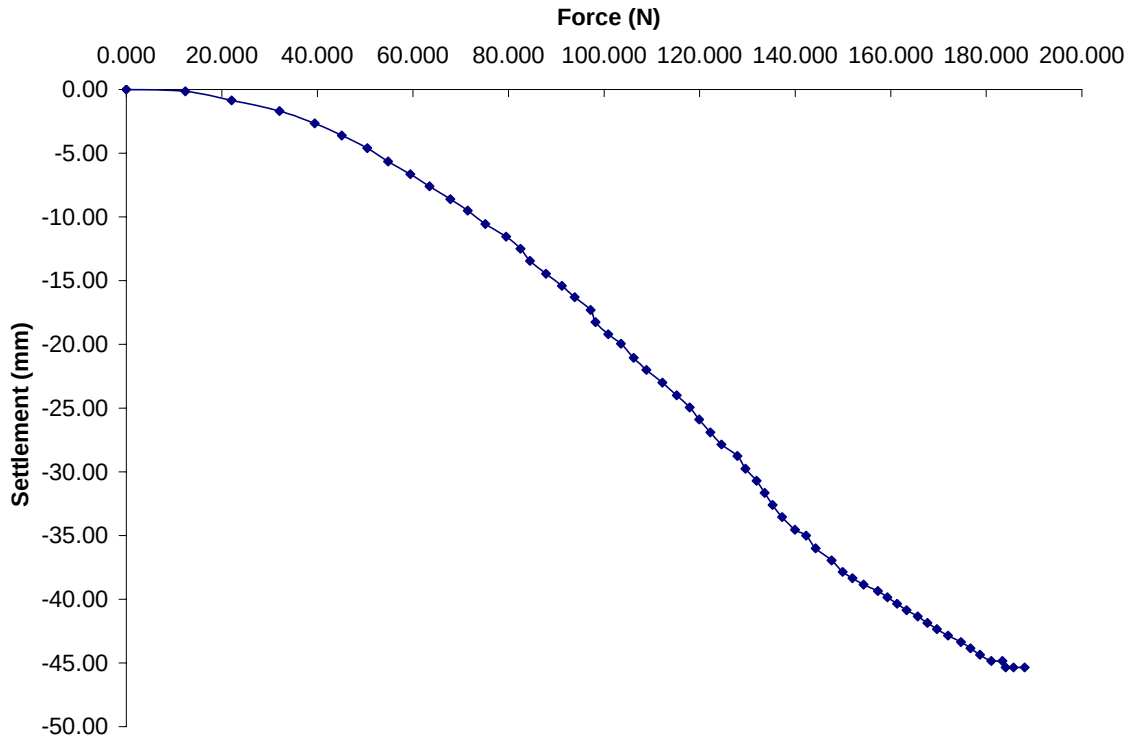

Figure 4.3 : The result of the axial force versus the settlement for Diamond Pattern

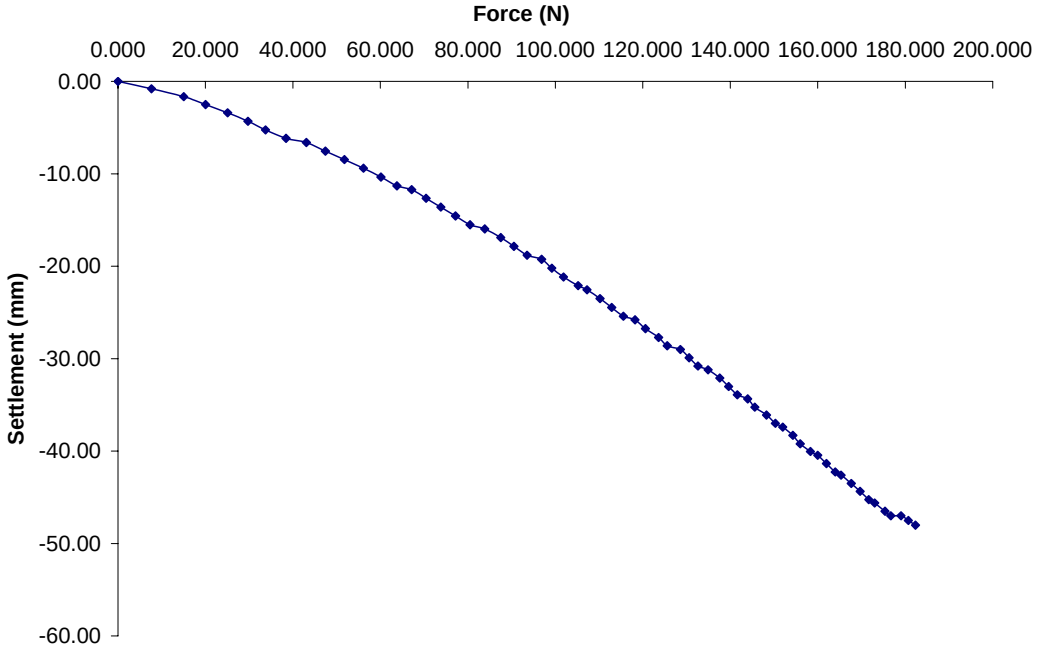

Figure 4.4 : The result of the axial force versus the settlement for Chevron Pattern

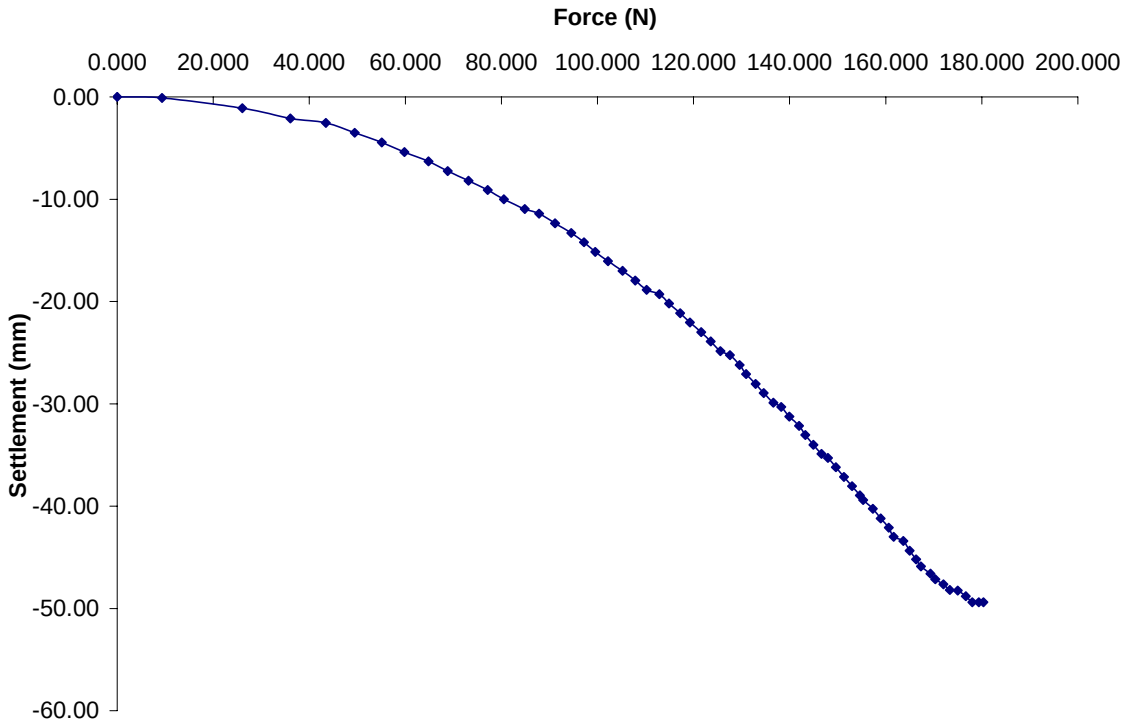

Figure 4.5 : The result of the axial force versus the settlement for Square Pattern

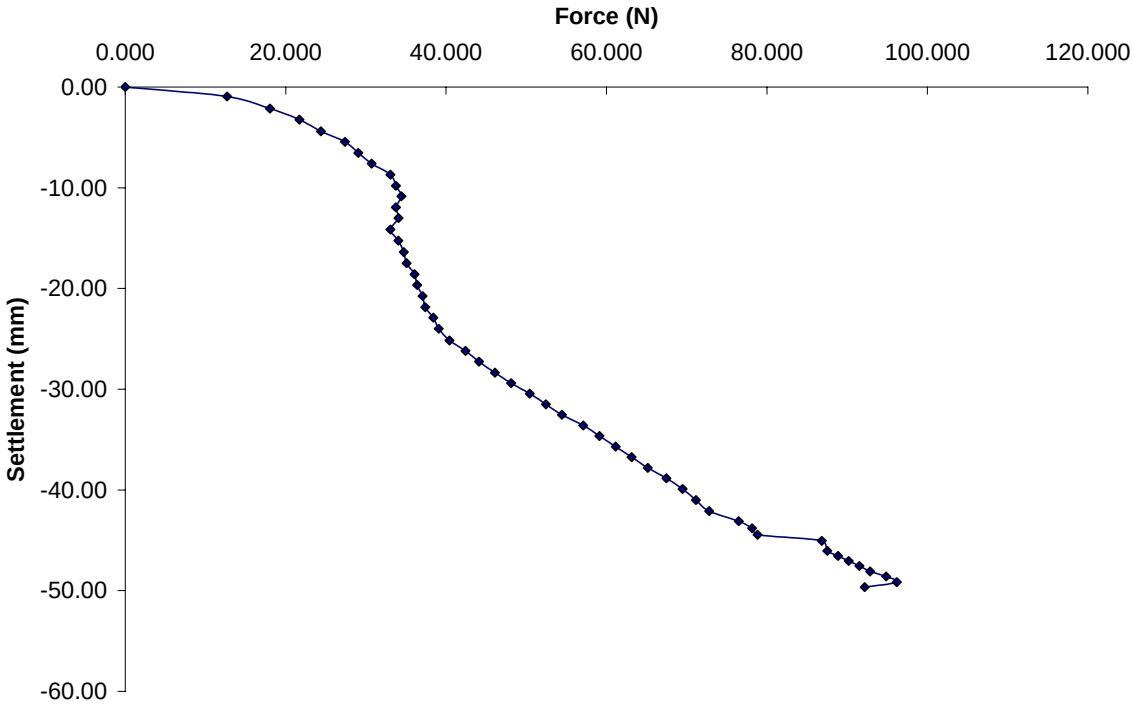

Figure 4.5 : The result of the axial force versus the settlement for Control (Non-Reinforced) sample

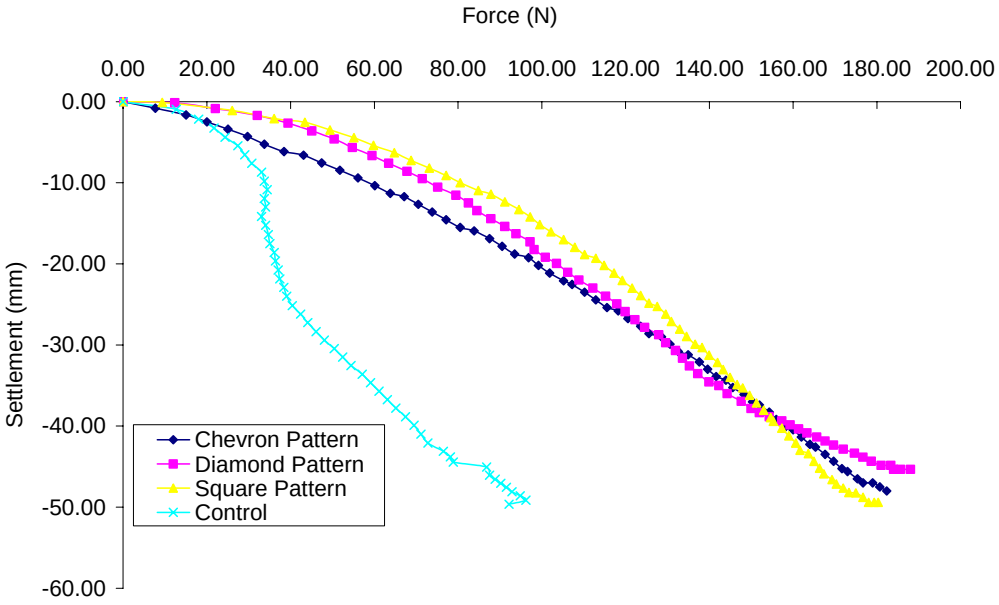

Figure 4.1 : The result of the axial force versus the settlement for All Tests

The constraint of the model test was the limitation of the maximum displacement of 50 mm for the LVDT used in the testing. Therefore, the interpretation and the discussion of the model test (in comparison to the control sample) are on the trend of the settlement curve versus axial force, for the settlement of less than 50 mm.

Figure 4.7 shows that all model tests exhibit similar trend of settlement curve with respect to the axial load. In comparison to the control sample, the grid mat models reduce the rate of the settlement, especially for the range of axial force of 30 N to 40 N. In addition, the control sample reached settlement of 49.6 mm at axial force of 92 N. While, the model tests samples reached 45 mm to 49 mm of settlement at axial force of 180 N to 188 N.

Beside that, Figure 4.7 shows that, for axial force of less than 120 N, the chevron model test produced higher settlement values than that of the square and the diamond pattern grid mats. This indicates that the chevron grid mat is less rigid than the square and the diamond pattern grid mats, which results in higher settlement values. For example, at 115 N axial force, the model test of the chevron pattern reaches 25 mm, whereby it can cause failure of the mat at 115 N, even though the maximum bearing capacity of the grid mat is about 182 N. Table 4.7 shows the maximum axial force values for the model test samples applied with diamond, chevron and square pattern grid mats, were of 180 N to 188 N.

Table 4.7 : Results of the testing

Pattern	**Maximum Axial Force (N)**	**Maximum Settlement (mm)**
Diamond	188.0	45.4
Chevron	182.4	48.0
Square	180.4	49.4
Control	92.2	49.7

Broms and Massarasch (1977) stated that for cohesive soils the ultimate bearing capacity of the grid (Q_{ult}) at penetration failure is dependent on the total surface are (A_m) of the individual cells in contact with the soil and on the adhesion c_a between the clay and the cell walls.

$Q_{ult} = c_a A_m$ for $c_u < 50$kPa

The adhesion c_a is dependent on the undrained shear strength c_u of the soil and on material of the grids. Experience from load tests with steel piles indicates that c_a can be 0.5 c_u when $c_u < 50$ kPa and as low as 10 kPa when $c_u > 50$ kPa. The scatter in the test results is large particularly when $c_u > 50$ kPa. Therefore the estimated ultimate bearing capacity for the each laboratory model sample was :

$Q_{ult} = c_a A_m$

$= (0.5c_u)(L \times B)$

$= 0.5 \times 12$ kN/m^2 x 0.175 m x 0.15 m

$= 0.158$ kN

$=$ **158 N**

The results of the maximum axial force for the laboratory model test samples were in good agreement with the estimated ultimate bearing capacity (Broms and Massarasch, 1977), with percentage differences of 14% to 19%. The grid mat model tests indicated the behavior of diamond pattern was superior to the grids with square and chevron pattern with respect to load carrying capacity, i.e., of 188 N versus 180 to 182 N.

CHAPTER 5

CONCLUSION AND RECOMMENDATIONS

5.1 Conclusion

A theoretical analysis and model tests indicate that the proposed new foundation grid which consists of thin-walled vertical plates has a high bearing capacity. The bearing capacity was approximately to that of a solid plate when the cells were filled with soil or had been pushed into the underlying soil.

The main purpose of the laboratory test was to produce higher bearing capacity in subgrade soil. Based on the objective and the result of the study, several conclusions can be made. The conclusion include the increase of the bearing capacity of the subgrade soil when grid mat are applied in the soil. In this study, one can also conclude that the shape of a grid mat influences the bearing capacity of the subgrade soil.

The experimental results showed that the diamond pattern of grid mat produced higher bearing capacity and a better settlement characteristic compared to that of the other patterns of grid mat models of the same sizes. This indicate that the chevron grid mat is less rigid than the square and the diamond pattern grid mats,

which results in higher settlement values. In other words, the grid mat with sufficient rigidity can prevent pre-mature failures (due to excessive settlement in the earlier phase of loading) before the ultimate bearing capacity of the subgred soil. The grid mat model tests indicate the behavior of diamond pattern was superior to the grids with square and chevron pattern with respect to load carrying capacity.

Grids can therefore be introduced as a new foundation type, if higher bearing capacity is to be achieved with lower settlement of the foundation. The result of this study show that the grid mat method can be used in practice, especially in the soft ground area. This will give another alternative for new foundation type in the construction engineering.

5.2 Recommendations For Future Research

There are several recommendations on the grid mat method for future works :

1. Modification of grid mat shapes like circular and triangular.
2. Modification of grid mat size, such as different size of the same shapes.
3. Effect of grid mat foundation on the lateral pressure along the circumference of the grid mat.

REFERENCES

Akinmusuru, 10. and Akinbolade, J. A, (1981. "Stability of Loaded Footings on Reinforced Soil." Journal of Geotechnical Engineering Devision, ASCE. Vol 107, pp 819-827.

Arenicz, R. M, (1992). "Effect of Reinforcement Layout on Soil Strength." Geotechnical Testing Journal, GTJODJ, vol 15 no 2, pp 158-165.

Bertok, J.(1987). " Settlement of Embankments and Structures at Vancouver International Airport." Journal of Canadian Geotechnic Vo124, pp 72-80.

Binquet, J., and Lee, Kenneth L,.(1976a). "Bearing Capacity Tests on Reinforced Earth Slabs." Journal of The Geotechnical Engineering Division, ASCE. Vol 101, pp 1241-1255.

Binquet, J., and Lee, Kenneth L,.(1976b). "Bearing Capacity Analysis of Reinforced Earth Slabs." Journal of The Geotechnical Engineering Division, ASCE. Vol 101, pp 1257-1276.

Broms, B.B and Massarch, K.R.(1977). "Grid Mats - A New Foundation Method." Proceeding of the ninth International Conference on Soil Mechanics and Foundation Engineering, Tokyo. Pp 433-438.

Bush, D. L, Jenner, C.G., and Basett. R. H., (1990), "The design and construction of a geocell foundation mattress supporting embankments over soft ground. Geotext. Geomembrane, volume 9, pp 83-98.

Capaccio, G., and Ward, I. M., (1974). "Properties of Ultra-high Modulus Linear Polypropylene". Nature Phys. Sci., Vol 243, pp 130-143.

Carter, G. R., and Dixon, J. H., (1995)., "Oriented polymer grid reinforcement". Construction and Building Materials, vol 9, No 6. pp 389-401

Casagrande, A. (1948). "Classification and Identification of Soil." Trans. ASCE, vol 113, pp 901-992.

Chalaturnyk, R.J., Scott, J. D., Chan, D. H. K.,and Richards, E. A. (1990). "Stress and Deformation in a Reinforced Soil Slope." Journal of Canadian Geotechnic Vo127, pp 224-232.

Cowland, J. W., and Wong, S.C.K., (1993). "Performance of a road embankment on soft clay supported on a geocell mattress foundation". Geotextiles and Geomembranes 12. pp 687-705.

Das, B.M.,(1999). " Principles Of Foundation Engineering ". Fourth Edition. Cole Publishing Company. pp 152-156.

Dash, S. K., Krishnaswamy, N. R., and Rajagopal, K., (2001)., "Bearing capacity of strip footings supported on geocell-reinforced sand". Geotextiles and Geomembranes no 19. pp 235-256.

De Garided et, R,. and Morel, G., (1986), "New strength techniques by textile elements fo low-volume roads". In Proc. Third Int. Conf, on Geotextiles. Vienna, Austria, pp 1027-1032.

Edgar, S., (1984)., "The Use of High Tensile Polymer Grid Mattress on the Musselburgh and Portobello Bypass", Proc. Engg. Polymer Grid Reinforcement in Civil Engr.,ICE, London, Paper #3.5.

Fatani, M. N., Bauer, G. E., and Al-Joulani, N.(1991). "Reinforcing Soil with Aligned and Randomly Oriented Metallic Fibers." Geotechnical Testing Journal, GTJODJ. Vol. 14 no 1, pp 78-87.

Gerald P. Raymond, (1992). "Reinforced Sand Behavior Overlying Compressible Subgrades" Journal of Geotechnical Engineering, ASCE Vol. 118, no 11, pp1663-1680.

Giroud, J. P., and Noiray, L., (1981). "Geotextile reinforced unpaved road design". Journal Geotech. Eng. Div. ASCE,107 GT9. pp 1233-1254.

Giroud, J. P., Ah-Line, C. and Bonaparte, N., (1984). " Design of unpaved Roads and Trafficked Area with Geogrid, " Proc. Symp. Polymer Grid Reinforcement in Civil Engineering, Mar 22-23, 1984. London. Pp

Haliburton, T. A., Anglin, C. C, and Lawmaster, J. D, (1978). "Testing of Geotechnical Fabric for Use as Reinforcement." Geotechnical Testing Journal, GTJODJ, vol 1 pp 203-212.

Hanna, A. and El-Rahman M.A.(1990). " Ultimate Bearing capacity of Triangular Shell Strip Footing on Sand." Journal of Geotechnical Engineering, ASCE. Vol 116 no 12, pp 1851-1862

Jarret, P. N., (1984)., "Evaluation of Geogrids for Construction of Roadways over Muskeg". Proc. Symp. Polymer Grid Reinforcement in Civil Engr., ICE, London.

Kazerani, B. and Jamnejad, G. H., (1987), "Polymer grid cell reinforcement in constructionof low cost highway" In Proc. Geosynthetic Conference. Vol 1 IFAI, USA, pp 58-68

Koerner, R. M, (1984). "Construction and Geotechnical Methods in Foundation Engineering". McGraw-Hill Book Co., New York.

Koerner, R. M, (1990). "Designing with Geosynthetics". Prentice Hall.

Krishnaswamy, N. R., Rajagopal, K., Latha, G. M., (2000). "Model studies on geocell supported embankment constructed over soft clay foundation". Geotechnical Testing Journal. No.23 vol. 1, pp 45-54. et. a11.

Kurian, N. P., and Mohan, C. S, (1981). "Contact Pressure Under Shell Foundation." Procceding 19^{rh} Int. Conf. for Soil Mechanics and Foundation Engineering, Stockholm. Sweden, pp165-168.

Leflive, E.,(1982) "The Reinforcement of Granular Materials with Continuous Fiber", Proc.2$^{°d}$ Int. Conf. on Geotextiles, Las Vegas, pp 721-726.

Leflive, E. and Liausu, Ph., ,(1986). " The Reinforcement of Soil by Continuous Thread ", Prod. 3`^{d} Int. Conf. on Geotextiles Vienna, pp 1159-1162.

Maher, M. H. and Ho, Y.C, (1993). "Behavior of Fiber-Reinforced Cemented Sand Under Static and Cyclic Loads." Geotechnical Testing Journal, GTJODJ. Vol. 16 no 3, pp 330-338.

Marto, A., and Khatib,A.(1999). "The Performance of Ribbed Raft Foundation Models in Clay Soil." Proceedings of the 5$^{t\prime}$ Geotechnical Engineering Conference (Geotropika 99), Johor Bahru, pp 177-188.

Marto, A., Yusuf, M. Z.. and Khatib,A.(2000). "The Efficiency of Ribbed Raft Foundation Models in Cohesive Soil." Proceedings of the 4^{b} Asia Pacific Structural Engineering and Construction Conference (APSEC 2000), Kuala Lumpur, pp 451-464.

McGown, A., Andrawes, K. Z., Hytiris, N and Mercer, F.B., (1985). "Soil Strengthening Using Random Distributed Mesh Element", Proc. 11$^{t\prime}$ ISSMFE Conf., Sanfransisco, pp 173 5-173 8.

Mhaiskar, S. Y and Mandal, J. N., (1996), "Investigation on soft clay subgrade strengthening using geocells". Construction and Building Materials, vol 10, No 4, pp 281-286.

Mitchel, J. K., Kao, T. C., Kavazanjiam, J. E., (1979)., "Analysis of grid cell reinforced pavement bases". Technical Report. No. GL-79-8, US Army Engineers Waterways Experiment station. July, 1979.

Miki, H. (1996). " Application of geosynthetics to embankment on soft ground and reclamation using soft soil ". Proceeding of the International syimposium on earth reinforcement. FukuokalKyushu/Japan, pp 919-942.

Milligan, G. W. E., and Love, J. P., (1984), "Model Testing of Geogrids Under an Aggregate Layer in Soft Ground, "Proc. Symp. Polymer Grid Reinfocement in Civil Engr, ICE, London. pp

Milligan, G. W. E., Jewell, R. A., Houlbsy, G. T., and Burd, H. J. (1989), "Anew approach to design of unpaved road Part I. Ground Eeng.,Apri125-29 1989.

Milovic, D. (1977). "Bearing Capacity Tests on Reinforced Sand." Proceeding of the ninth International Conference on Soil Mechanics and Foundation Engineering, Tokyo. Pp 651-654.

Min, Y., Leshchinsky, D., Ling, H. L, and Kaliakin, N. V. (1995). "Effect of Suistained and Repeated Tensile Loads on Geogrid Embedded in Sand." Geotechnical Testing Journal, GTJODJ, vol. 18, no. 2 pp, 204-225.

Nagaraju, S. S., and Mhaiskar, S. Y., (1983)., "Experiment on the use of geotextile and geocomposites in paved roads. In Proc. Indian Geotechnical Conference. Vol 1, Indian Geotechnical Society. Pp 89-92.

Netlon Ltd, (1996). "Technical Literature". Blackburn, UK.

Oda, M. and Win,Soe. (1990). "Ultimate Bearing Capacity Test on Sand with Clay Layer." Journal of Geotechnical Engineering, ASCE. Vol 116 no 12, pp 1902-1907.

Omar M. T, Das,B. M, and Yen, S. C, (1993). "IJltimate Bearing Capacity of Shallow Foundation on Sand with Geogrid Reinforcement." Journal of Canadian Geotechnic Vol 30, pp 545-549.

Rea, C., Mitchel, J. K., (1978)." Sand reinforcement using paper grid cells, Reprint 3130, ASCE spring convention and exhibit. Pittsbrugh, PA, pp 24-28.

Richardson, G. N.,and Lee, K. L, (1975)"Seismic Design of Reinforced Earth Walls." Journal of the Geotechnical Engineering Division, ASCE, vol 101, pp 167-188.

Robertson, J., and Gilchrist, A. J. T. (1987), "Design and construction of a reinforced embankment across soft lakebed deposites".Ing. Conf. on Foundation and Tunels.

Rowe, R.K, and Mylleville Brian, L. J, (1993). "The Stability of Embankments Reinforced with Steel." Journal of Canadian Geotechnic Vo130, pp 768-780.

Schimizu, M.., and Innui, T., (1990). "Increase in bearing capacity of ground with geotxtile wall frame". Proccedings of the fourth International Conference on Geotextiles Geomenbranes and Related Products, vol. 1.Hague, Netherlands. p. 254.

Sellmeijer, J. B., Kenter, C. J, and Van den Berg, J., (1982), "Calculation method for a fabric reinforced road.,Proc. Second International Conference on Geotextiles, Lasvegas, A. A. Balkema, Rotterdam, pp 393-398.

Shenbaga R.Kaniraj, (1988). "Design of Reinforced Embankments on Soft Soils' Journal of Geotechnical Engineering. Vol. 19, pp 127-142.

Shin, E.C, Das, B. M, Puri, V. K, Yen, S. C and Cook, E. E, (1993). "Bearing Capacity of Strip Foundation on Geogrid-Reinforced." Geotechnical Testing Journal, GTJODJ, vol 16, no 4 pp 534-541.

Tatsouka, F. and Leshchinsky, D. (1993). "Recent Case Histories of Permanent Geosynthetic-Reinforced Soil Retaining Walls." Procceding, Geosyinthetic,Conference, Atlanta, pp.87-100.

Terzaghi, K., Ralph B. Peck and Cholamreza Mesri, (1996). "Soil Mechanics in Engineering Practice." John Wiley & Sons, Inc, pp 27-28.

U. S. Army Res. Dev. Acquisition Mag., (1981)., "WES Developing Sand-Grid Confinement System". P 7.

Verma, BY and Char, A. N. R, (1986). "Bearing Capacity Test on Reinforced Sand Subgrade." Journal of Geotechnical Engineering, ASCE. Vol 112, pp 1701-706.

Vesic, A. (1963). "Bearing Capacity of Deep Foundation in Sand." Highway., Res. Rec., No 39, Nat, Academy of Sci., Nat. Res Concil. Washington, D.C, pp

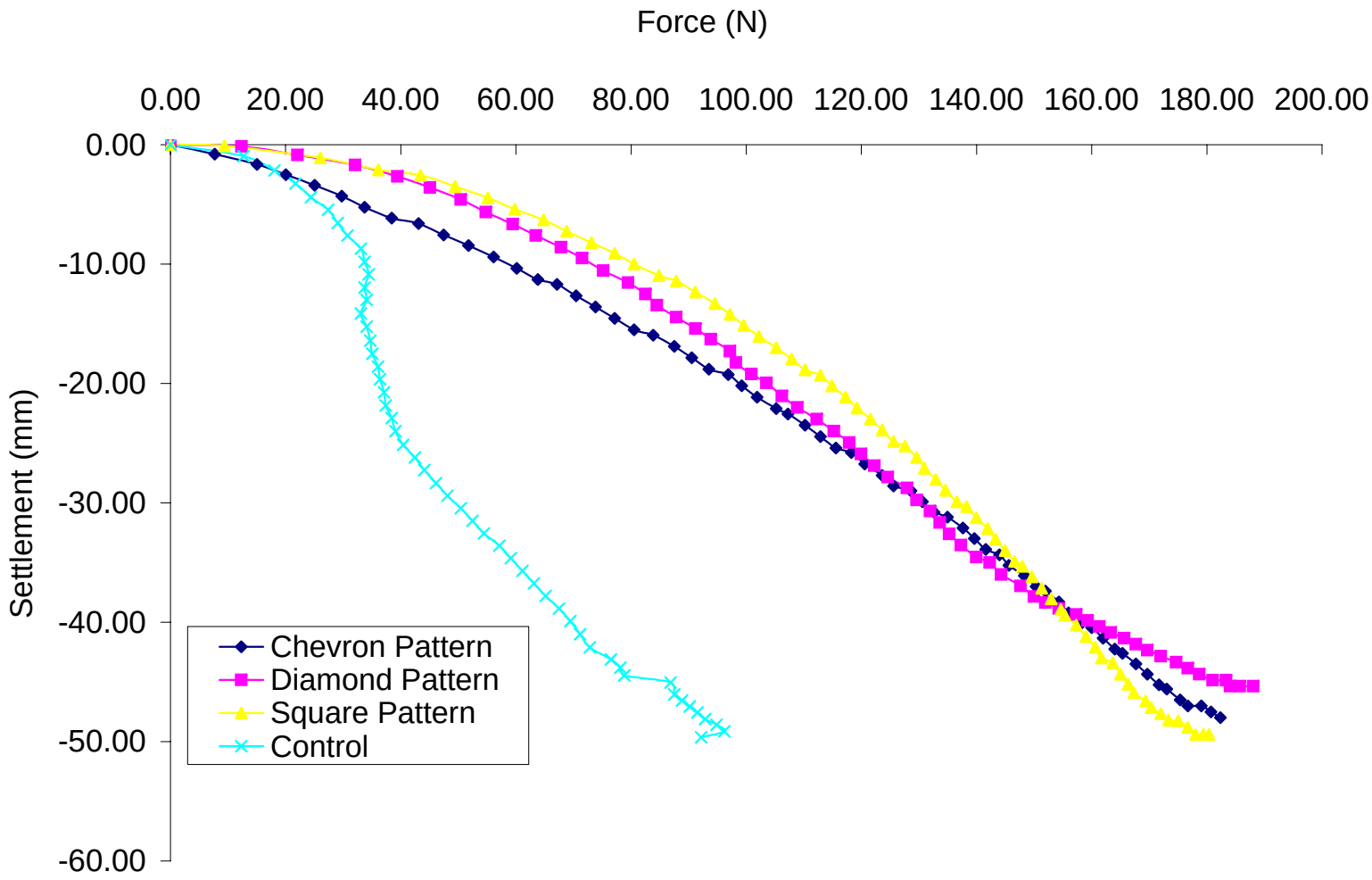
Force (N)
0.00
20.00
40.00
60.00
80.00
100.00
120.00
140.00
160.00
180.00
200.00
Settlement (mm)
0.00
-10.00
-20.00
-30.00
-40.00
-50.00
-60.00
Chevron Pattern
Diamond Pattern
Square Pattern
Control

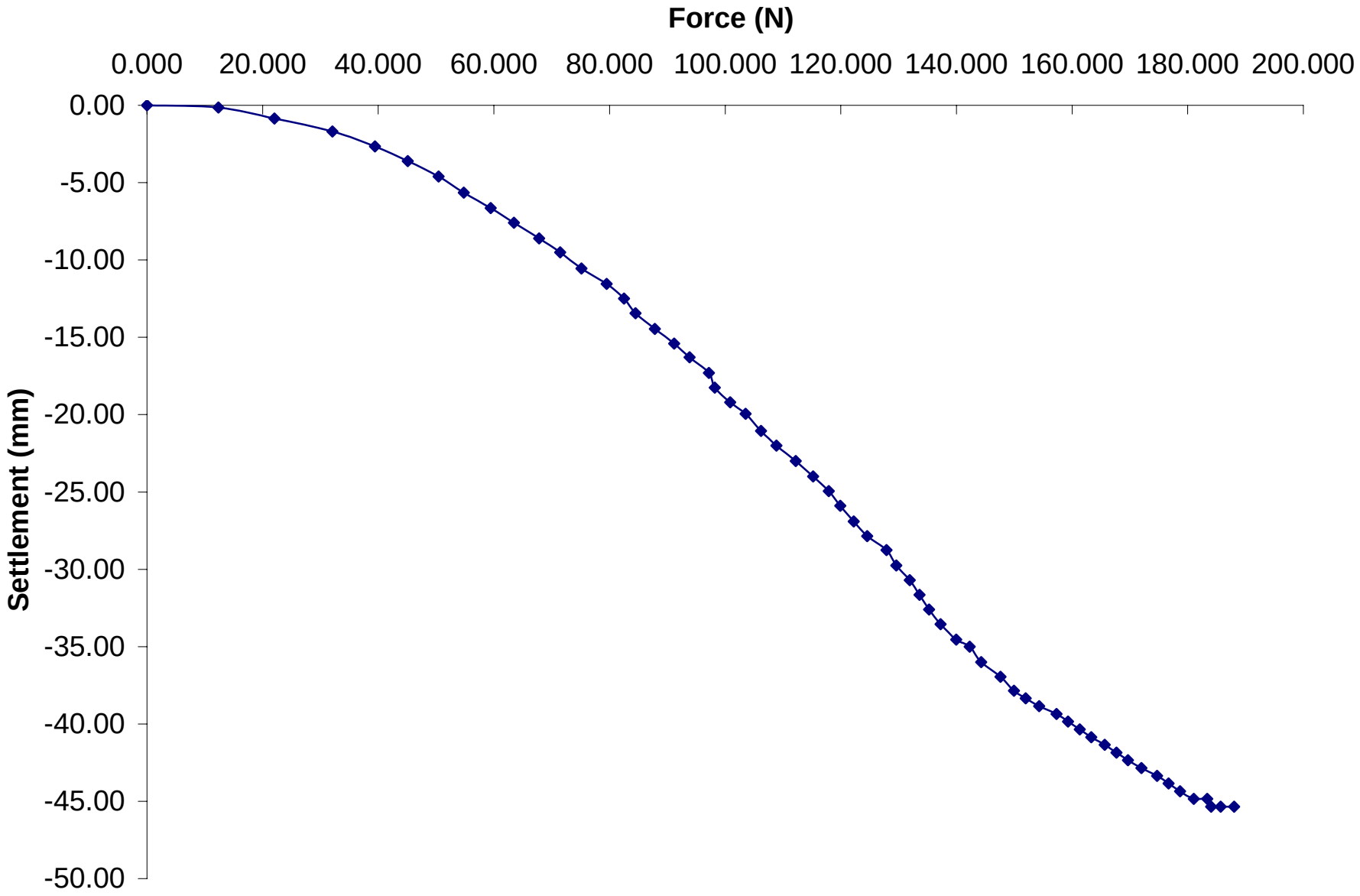
Force (N)
0.000
20.000
40.000
60.000
80.000
100.000
120.000
140.000
160.000
180.000
200.000
Settlement (mm)
0.00
-5.00
-10.00
-15.00
-20.00
-25.00
-30.00
-35.00
-40.00
-45.00
-50.00

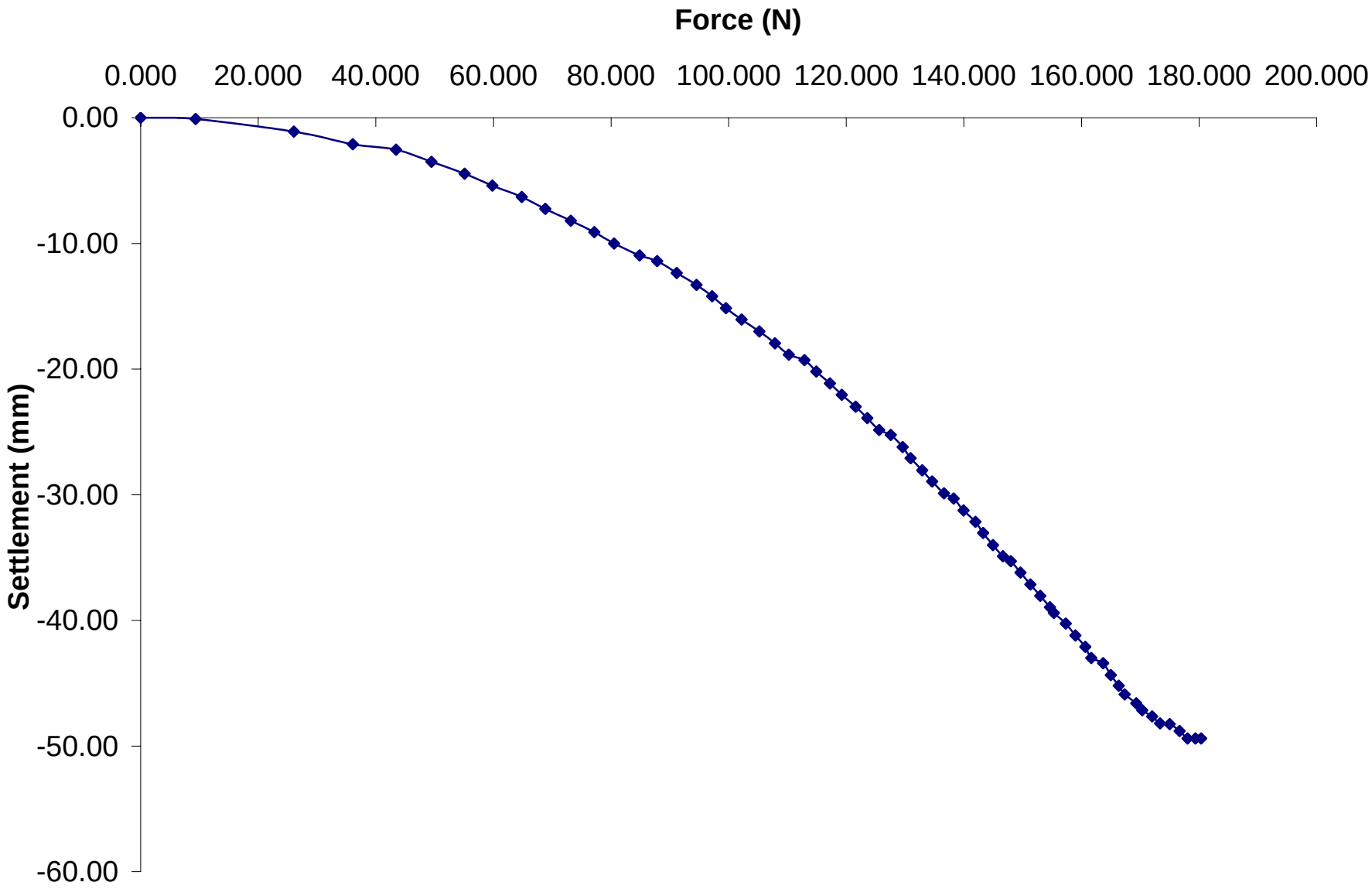
Force (N)
0.000
20.000
40.000
60.000
80.000
100.000
120.000
140.000
160.000
180.000
200.000
Settlement (mm)
0.00
-10.00
-20.00
-30.00
-40.00
-50.00
-60.00

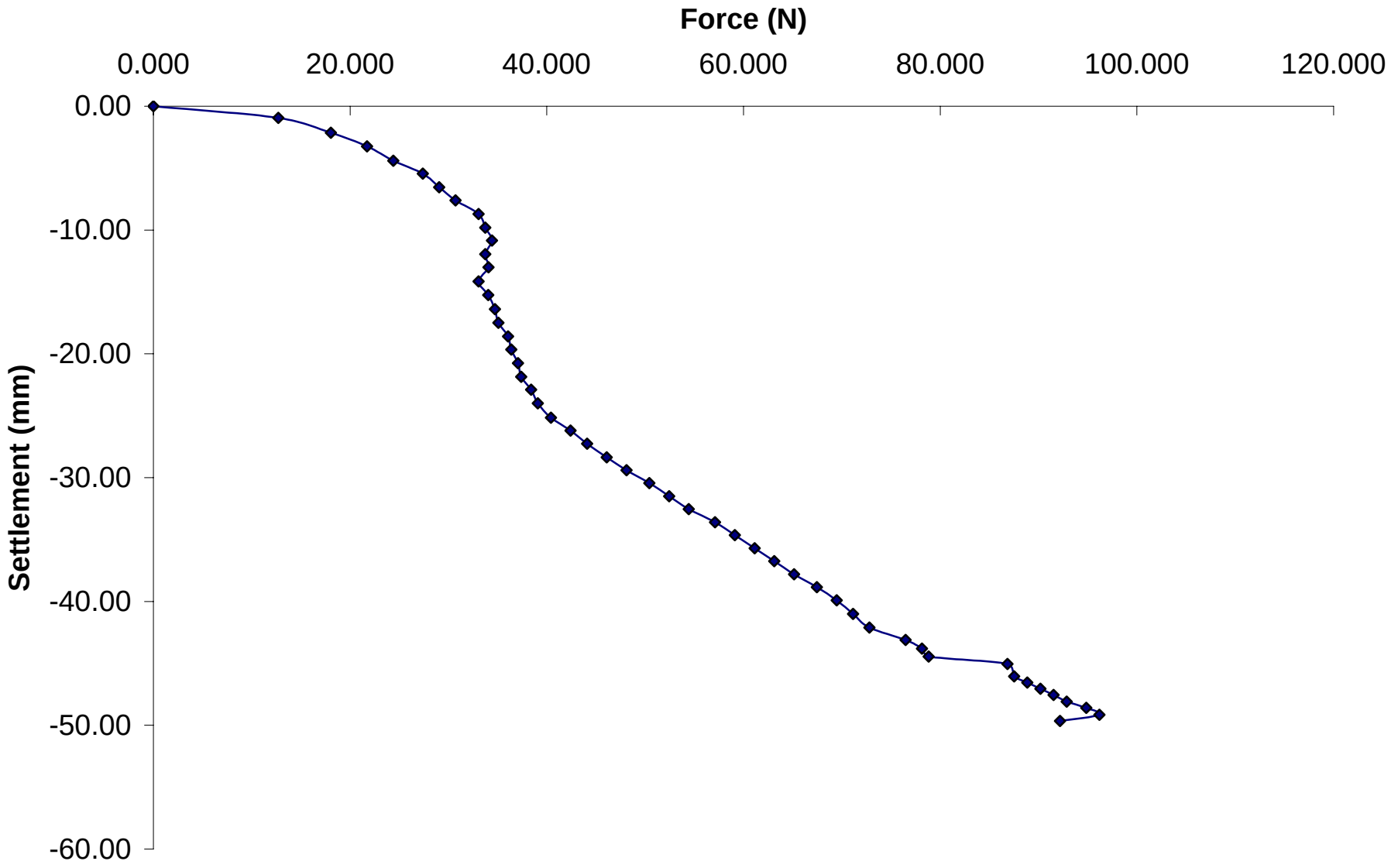
Force (N)
0.000
20.000
40.000
60.000
80.000
100.000
120.000
Settlement (mm)
0.00
-10.00
-20.00
-30.00
-40.00
-50.00
-60.00